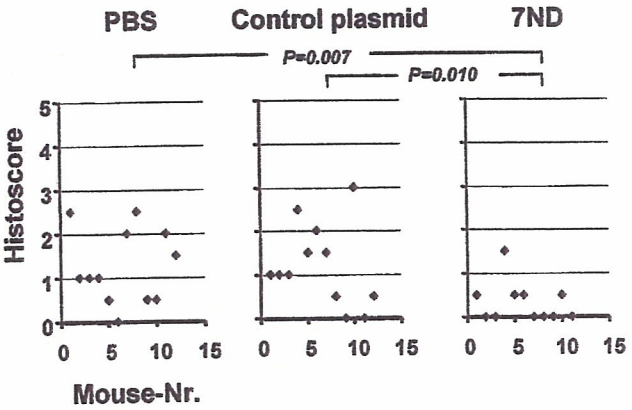

Figure 5. Anti-MCP-1 gene therapy: effects on the severity and prevalence of myocarditis. *P<0.05.

IFN-γ and IL-10 (compared with control plasmid-treated and PBS-treated mice) was significantly increased (Figure 6a). Inhibition of MCP-1 with 7ND gene transfection also reduces mRNA expression levels of the chemokines RANTES, MIP-2, IP-10, MCP-1, TCA-3, and eotaxin in the myocardium (Figure 6b).

Discussion

We have shown an important role for MCP-1 and MIP1-α and their major receptors, CCR2 and CCR5, in the initiation of the autoimmune myocarditis. Not only blocking MCP-1 and MIP1-α by using monoclonal antibodies but also by immunizing CCR2−/− and CCR5−/− mice reduced the severity of myocarditis. Furthermore, we demonstrated successful gene therapy by blocking MCP-1 activity in vivo by using an N-terminal deletion mutant of MCP-1 called 7ND. Because it lacks the N-terminal amino acid 2 to 8 and blocks MCP-1–mediated monocyte chemotaxis,[8,9] it is effective in the treatment of EAM in mice. In contrast, the control gene had no significant effect on disease severity. Immunizing CCR2−/− mice and treating BALB/c mice with 7ND resulted in significantly decreased IL-1 and IL-4 and in significantly increased IL-10 and IFN-γ production by splenocytes. In addition, mRNA expression levels of the chemokines RANTES, MIP-2, IP-10, MCP-1, TCA-3, and eotaxin in the myocardium were especially reduced in 7ND-treated mice. Overall, these findings indicated a critical role in the inflammatory response of myocarditis and further suggest that a mutant MCP-1 can be used as a novel therapeutic approach for the treatment of human autoimmune myocarditis.

MCP-1, MIP1-α, and their major receptors, CCR2 and CCR5, play important roles in the pathogenesis of many inflammatory diseases.[15–17] MCP-1 mRNA expression has been shown in endomyocardial biopsy specimens from patients with dilated cardiomyopathy, suggesting an important role of this chemokine in the regulation of inflammatory cell infiltration into the myocardium.[18]

Blocking both MCP-1 or MIP-1α with mAbs before the onset of inflammation, which occurs after day 14 in our model of EAM, led to significant reduction of the severity of myocarditis in BALB/c mice immunized with cardiac myosin. Similar results were obtained when CCR2- and CCR5-deficient mice were immunized. Additionally, in CCR5-deficient mice, the cardiac myosin–specific production of IL-10 by splenocytes was increased and the production of TNF-α was reduced significantly. The production of IL-2 and IFN-γ were also slightly reduced in CCR5-deficient mice, but the differences were not significant. Our results conform with the reported studies that CCR5 is expressed mostly on Th1 lymphoctes.[19] In our studies with CCR5-deficient mice, the Th2 cytokine IL-10 was significantly increased and the Th1-associated cytokines tumor necrosis factor-α (TNF-α) significantly and IL-2 and IFN-γ (not significantly) were reduced. Because it is known that the EAM in BALB/c mice is a Th1-induced disease,[20] this along with the inhibition of

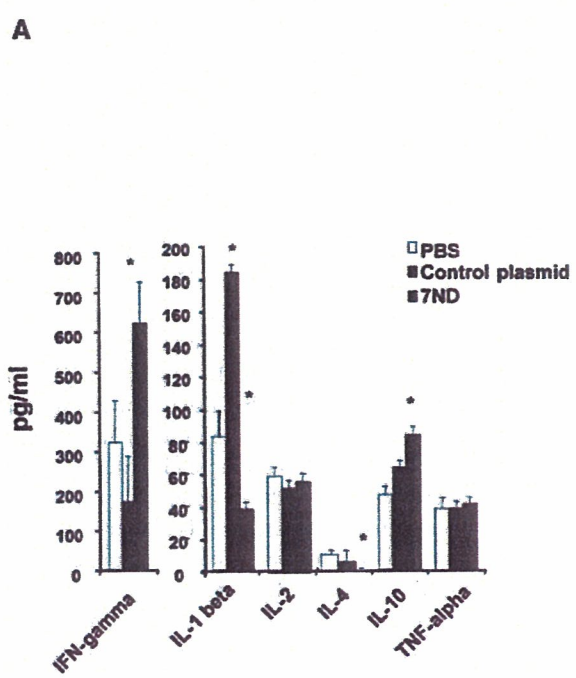

Figure 6. Anti–MCP-1 gene therapy. A, Effect on cytokine production by splenocytes after cardiac myosin stimulation at day 21. B, RNA protection assay. mRNA expression levels of the some chemokines in the myocardium of either 7ND-, control plasmid-, or PBS-treated mice on day 21. *P<0.05.

cell migration might be an additional explanation for the reduction in the myocarditis score in CCR5-deficient mice. In CCR2-deficient mice, the cardiac myosin–specific production of IL-1 and IL-4 by splenocytes was reduced significantly, whereas the production of IFN-γ was increased. CCR2 is known to be expressed on both Th1 and Th2 lymphoctes.[19] In our previous work, we have shown that IFN-γ and IL-10 are protective cytokines in myocarditis, whereas IL-1 and TNF-α promote inflammation and disease severity in EAM.[12,21,22] We further studied the expression of different CCRs during inflammation in the myocardium of mice and questioned whether there is a upregulation of other chemokine receptors in CCR2- or CCR5-deficient mice, and we found that mainly CCR1, CCR2, and CCR5 are expressed in the myocardium, with no or very low expression of mRNA for the receptors CCR3 and CCR4. Further, the CCR2- and CCR5-deficient mice did not show marked upregulation of the other CCRs tested compared with the wild-type mice. Finally, we studied the mRNA expression levels of other chemokines in the myocardium of these mice on day 21 and found that the cytokines RANTES, MIP-2, IP-10, and MCP-1 were especially expressed in the myocardium in all tested mice. The mRNA expression levels of these chemokines correlated with the severity of myocarditis and were independent of CCR2 or CCR5 expression. Thus, the expression of these chemokines was continuously lower in CCR2- and CCR5-deficient mice (with overall mild to no inflammation), but with differences in the wild-type mice by means of higher mRNA expression levels in mice with higher myocarditis score, indicating that these chemokines were mostly released by the myocardium migrating inflammatory cells during the inflammation.

Fuse and colleagues[7] showed increased mRNA levels of MCP-1 in the hearts of rats immunized with cardiac myosin and significantly elevated serum MCP-1 levels of the rats with EAM from days 15 until 24. Furthermore, Kolattukudy and colleagues[23] were able to induce myocarditis in mice by targeted expression of the MCP-1 gene in murine cardiac muscle. Damas and colleagues[24] demonstrated that MCP-1 can directly affect cardiomyocytes and showed that MCP-1 can modulate cytokine production within the myocardium by significantly increasing both IL-1b and IL-6 production in cardiomyocytes. They have further shown increased gene expression of the MCP-1 receptor (CCR2) in the failing human myocardium.[25] Besides chemotaxis and leukocyte activation, MCP-1 and other chemokines may also regulate several other biological processes with importance to the pathogenesis of heart failure, such as fibrosis, angiogenesis, and apoptosis.[26]

Determining the appropriate treatment of autoimmune myocarditis still remains a major clinical problem. Immunomodulatory therapies have been used in clinical trials for the treatment of myocarditis.[27] However, clinical trials and experimental studies of murine models of myocarditis have yet not established a generally accepted immunosuppressive treatment of autoimmune myocarditis. We obtained promising results by blocking MCP-1 or MIP-1α in vivo. Because MCP-1 and MIP-1α act through different pathways, blocking them together may even have an additive or synergetic effect. Gene therapy to block MCP-1 activity in vivo by using an N-terminal deletion mutant of MCP-1 is another possibility. Recently, Egashira and colleagues[28] demonstrated that mutant MCP-1 7ND protein secreted from the transfected skeletal muscle cells into the circulation blood blocks the MCP-1/CCR2 signal pathway in remote target organs or tissue and suppresses monocyte recruitment. This 7ND gene construct has been used successfully in treatment of several other inflammatory diseases.[13,14] Further 7ND treatment had no negative effect on the clearance of coxsackievirus B3 in our study, which might be important for future clinical trials, as the myocarditis seen in humans is mostly virus-induced and latent virus may be present (Kaya et al, unpublished data, 2005).

There are a number of mechanisms by which blocking MCP-1 may affect the development of myocarditis. Although the pathogenesis of myocarditis has not yet been fully elucidated, the migration of antigen-specific T cells in the myocardium is considered to be the initial process. Subsequently, large numbers of inflammatory cells infiltrate into the myocardium, including non–antigen-specific T cells, B cells, macrophages, and neutrophils that elicit full-blown myocarditis. In the latter process, chemoattractants play a major role in the recruitment of inflammatory cells. Fuse et al[7] demonstrated an abrupt onset and serum levels of MCP-1 elevated simultaneously with the onset of the disease. The expression of MCP-1 mRNA also coincided with the onset of EAM. MCP-1 is a potent chemotactic factor for mononuclear cells. Thus, the inflammatory infiltrate observed in myocardial lesions of myocarditis consists of >70% mononuclear cells.[10]

Proinflammatory cytokines are important in the development of autoimmune myocarditis. Administration of IL-1 or TNF-α promoted virus- and myosin-induced myocarditis in genetically resistant B10.A mice.[22] In addition, when A/J mice are infected with CB3 and treated with an IL-1 receptor antagonist, myocardial injury is diminished.[29] Thus, IL-1 and TNF-α are critical in the pathogenesis of autoimmune myocarditis. Both cytokines can upregulate major histocompatibility complex class I and class II expression in the cardiac interstitium and on myocytes, possibly inducing or enhancing inflammation. Cardiomyocytes stimulated in vitro by MCP-1 are able to produce proinflammatory cytokines such IL-1,[24] which in turn may reduce cardiomyocyte contractility and increase cardiac hypertrophy.[30,31] IL-1 in turn may induce MCP-1 production in several cell types.[32] Accordingly, in CCR2−/− mice immunized with cardiac myosin and in mice treated with 7ND, there was significantly less infiltration, including all cell types, in the heart sections, significantly reduced cardiac myosin-specific production of IL-1 and IL-4 and increased production of IL-10 and IFN-γ. Recently, we showed that IL-4 promotes the disease in EAM and IFN-γ limits it. Suppression of IFN-γ represents at least one of the mechanisms by which IL-4 promotes EAM.[33] Lack of IFN-γ due to either depletion with an antibody or a genetic deficiency exacerbated myocarditis. Treatment of mice with recombinant IFN-γ suppressed the development of myocarditis. Thus, IFN-γ has a disease-limiting effect in EAM.[21] IL-10 is primarily produced by monocytes and T cells and plays an important role in controlling cell-mediated and

inflammatory responses, including EAM.[12] IL-10 also suppresses inflammatory responses in cardiomyocytes by reducing TNF-α–stimulated release of MCP-1. Although TNF-α has no effect on IL-10 and only modest effects on IL-1 and IL-6 levels in adult rat cardiomyocytes, this cytokine is a potent inducer of MCP-1 in these cells.[24] However, there is strain and species-specific difference in myocarditis with regard to Th1 and Th2 and the promotion of cardiac inflammation.[20,33,34]

There appears to be no compensatory upregulation of other chemokines when blocking MCP-1 with the 7ND construct. In contrast, mice treated with 7ND showed significant reduction in other chemokines such as RANTES, MIP-2, IP-10, MCP-1, TCA-3, and eotaxin, all chemokines that can be produced by different inflammatory cells locally during an inflammation and thus aggravate inflammation. Therefore, reducing the migration of inflammatory cells by blocking MCP-1 not only leads to reduced inflammatory cells in the myocardium but also reduced production of additional chemokine production in the myocardium.

Overall, these findings suggest that MCP-1 and MIP-1α, acting through their receptors CCR2 and CCR5, are important in the induction of EAM and that inhibition of MCP-1 with 7ND gene transfection significantly reduced the disease severity. This strategy may be a new feasible form of gene therapy against autoimmune myocarditis.

Acknowledgments

This work was supported by the Deutsche Herzstiftung and in part by the National Institutes of Health grants HL67290 and HL70729. The authors thank Florian Leuschner, Theresa Tretter, and Özay Kaya for critically reading the manuscript.

References

1. Rollins BJ. Chemokines Blood. 1997;90:909–928.
2. Koch AE, Kunkel SL, Harlow LA, Mazarakis DD, Haines GK, Burdick MD, Pope RM, Strieter RM. Macrophage inflammatory protein-1 alpha: a novel chemotactic cytokine for macrophages in rheumatoid arthritis. J Clin Invest. 1994;93:921–928.
3. Carr MW, Roth SJ, Luther E, Rose SS, Springer TA. Monocyte chemoattractant protein 1 acts as a T-lymphocyte chemoattractant. Proc Natl Acad Sci U S A. 1994;91:3652–3656.
4. Gu L, Tseng S, Horner RM, Tam C, Loda M, Rollins BJ. Control of TH2 polarization by the chemokine monocyte chemoattractant protein-1. Nature. 2000;404:407–411.
5. Sallusto F, Mackay CR, Lanzavecchia A. The role of chemokine receptors in primary, effector, and memory immune responses. Annu Rev Immunol. 2000;18:593–620.
6. Caforio AL, Mahon NJ, McKenna WJ. Cardiac autoantibodies to myosin and other heart-specific autoantigens in myocarditis and dilated cardiomyopathy. Autoimmunity. 2001;34:199–204.
7. Fuse K, Kodama M, Hanawa H, Okura Y, Ito M, Shiono T, Maruyama S, Hirono S, Kato K, Watanabe K, Aizawa Y. Enhanced expression and production of monocyte chemoattractant protein-1 in myocarditis. Clin Exp Immunol. 2001;124:346–352.
8. Zhang YJ, Rutledge BJ, Rollins BJ. Structure/activity analysis of human monocyte chemoattractant protein-1 (MCP-1) by mutagenesis: identification of a mutated protein that inhibits MCP-1-mediated monocyte chemotaxis. J Biol Chem. 1994;269:15918–15924.
9. Zhang Y, Rollins BJ. A dominant negative inhibitor indicates that monocyte chemoattractant protein 1 functions as a dimer. Mol Cell Biol. 1995;15:4851–4855.
10. Pummerer C, Berger P, Fruhwirth M, Ofner C, Neu N. Cellular infiltrate, major histocompatibility antigen expression and immunopathogenic mechanisms in cardiac myosin-induced myocarditis. Lab Invest. 1991; 65:538–547.
11. Kaya Z, Afanasyeva M, Wang Y, Dohmen KM, Schlichting J, Tretter T, Fairweather D, Holers VM, Rose NR. Contribution of the innate immune system to autoimmune myocarditis: a role for complement. Nat Immunol. 2001;2:739–745.
12. Kaya Z, Dohmen KM, Wang Y, Schlichting J, Afanasyeva M, Leuschner F, Rose NR. Cutting edge: a critical role for IL-10 in induction of nasal tolerance in experimental autoimmune myocarditis. J Immunol. 2002; 168:1552–1556.
13. Ni W, Egashira K, Kitamoto S, Kataoka C, Koyanagi M, Inoue S, Imaizumi K, Akiyama C, Nishida KK, Takeshita A. New anti-monocyte chemoattractant protein-1 gene therapy attenuates atherosclerosis in apolipoprotein E-knockout mice. Circulation. 2001;103:2096–2101.
14. Shimizu S, Nakashima H, Masutani K, Inoue Y, Miyake K, Akahoshi M, Tanaka Y, Egashira K, Hirakata H, Otsuka T, Harada M Anti-monocyte chemoattractant protein-1 gene therapy attenuates nephritis in MRL/lpr mice. Rheumatology (Oxford). 2004;43:1121–1128.
15. Rao AR, Quinones MP, Garavito E, Kalkonde Y, Jimenez F, Gibbons C, Perez J, Melby P, Kuziel W, Reddick RL, Ahuja SK, Ahuja SS. CC chemokine receptor 2 expression in donor cells serves an essential role in graft-versus-host-disease. J Immunol. 2003;171:4875–4885.
16. Ni W, Kitamoto S, Ishibashi M, Usui M, Inoue S, Hiasa K, Zhao Q, Nishida K, Takeshita A, Egashira K. Monocyte chemoattractant protein-1 is an essential inflammatory mediator in angiotensin II-induced progression of established atherosclerosis in hypercholesterolemic mice. Arterioscler Thromb Vasc Biol. 2004;24:534–539.
17. Bruhl H, Cihak J, Schneider MA, Plachy J, Rupp T, Wenzel I, Shakarami M, Milz S, Ellwart JW, Stangassinger M, Schlondorff D, Mack M. Dual role of CCR2 during initiation and progression of collagen-induced arthritis: evidence for regulatory activity of CCR2+ T cells. J Immunol. 2004;172:890–898.
18. Lehmann MH, Kuhnert H, Muller S, Sigusch HH. Monocyte chemoattractant protein 1 (MCP-1) gene expression in dilated cardiomyopathy. Cytokine. 1998;10:739–746.
19. Bonecchi R, Bianchi G, Bordignon PP, D'Ambrosio D, Lang R, Borsatti A, Sozzani S, Allavena P, Gray PA, Mantovani A, Sinigaglia F. Differential expression of chemokine receptors and chemotactic responsiveness of type 1 T helper cells (Th1s) and Th2s. J Exp Med. 1998;187:129–134.
20. Smith SC, Allen PM. Myosin-induced acute myocarditis is a T cell-mediated disease. J Immunol. 1991;147:2141–2147.
21. Afanasyeva M, Wang Y, Kaya Z, Stafford EA, Dohmen KM, Sadighi Akha AA, Rose NR. Interleukin-12 receptor/STAT4 signaling is required for the development of autoimmune myocarditis in mice by an interferon-gamma-independent pathway. Circulation. 2001;104:3145–3151.
22. Lane JR, Neumann DA, Lafond-Walker A, Herskowitz A, Rose NR. Interleukin 1 or tumor necrosis factor can promote Coxsackie B3-induced myocarditis in resistant B10.A mice. J Exp Med. 1992;175:1123–1129.
23. Kolattukudy PE, Quach T, Bergese S, Breckenridge S, Hensley J, Altschuld R, Gordillo G, Klenotic S, Orosz C, Parker-Thornburg J. Myocarditis induced by targeted expression of the MCP-1 gene in murine cardiac muscle. Am J Pathol. 1998;152:101–111.
24. Damas JK, Aukrust P, Ueland T, Odegaard A, Eiken HG, Gullestad L, Sejersted OM, Christensen G. Monocyte chemoattractant protein-1 enhances and interleukin-10 suppresses the production of inflammatory cytokines in adult rat cardiomyocytes. Basic Res Cardiol. 2001;96: 345–352.
25. Damas JK, Eiken HG, Oie E, Bjerkeli V, Yndestad A, Ueland T, Tonnessen T, Geiran OR, Aass H, Simonsen S, Christensen G, Froland SS, Attramadal H, Gullestad L, Aukrust P. Myocardial expression of CC- and CXC-chemokines and their receptors in human end-stage heart failure. Cardiovasc Res. 2000;47:778–787.
26. Weber KS, Nelson PJ, Grone HJ, Weber C. Expression of CCR2 by endothelial cells: implications for MCP-1 mediated wound injury repair and in vivo inflammatory activation of endothelium. Arterioscler Thromb Vasc Biol. 1999;19:2085–2093.
27. Mason JW, O'Connell JB, Herskowitz A, Rose NR, McManus BM, Billingham ME, Moon TE. A clinical trial of immunosuppressive therapy for myocarditis: the Myocarditis Treatment Trial Investigators. N Engl J Med. 1995;333:269–275.
28. Egashira K, Koyanagi M, Kitamoto S, Ni W, Kataoka C, Morishita R, Kaneda Y, Akiyama C, Nishida KI, Sueishi K, Takeshita A. Anti-monocyte chemoattractant protein-1 gene therapy inhibits vascular remodeling in rats: blockade of MCP-1 activity after intramuscular transfer of a mutant gene inhibits vascular remodeling induced by chronic blockade of NO synthesis. FASEB J. 2000;14:1974–1978.

29. Lane JR, Neumann DA, Lafond-Walker A, Herskowitz A, Rose NR. Role of IL-1 and tumor necrosis factor in coxsackie virus-induced autoimmune myocarditis. J Immunol. 1993;151:1682–1690.
30. Gulick T, Chung MK, Pieper SJ, Lange LG, Schreiner GF. Interleukin 1 and tumor necrosis factor inhibit cardiac myocyte beta-adrenergic responsiveness. Proc Natl Acad Sci U S A. 1989;86:6753–6757.
31. Hirota H, Chen J, Betz UA, Rajewsky K, Gu Y, Ross J Jr, Muller W, Chien KR. Loss of a gp130 cardiac muscle cell survival pathway is a critical event in the onset of heart failure during biomechanical stress. Cell. 1999;97:189–198.
32. Yamamoto T, Eckes B, Mauch C, Hartmann K, Krieg T. Monocyte chemoattractant protein-1 enhances gene expression and synthesis of matrix metalloproteinase-1 in human fibroblasts by an autocrine IL-1 alpha loop. J Immunol. 2000;164:6174–6179.
33. Afanasyeva M, Wang Y, Kaya Z, Park S, Zilliox MJ, Schofield BH, Hill SL, Rose NR. Experimental autoimmune myocarditis in A/J mice is an interleukin-4-dependent disease with a Th2 phenotype. Am J Pathol. 2001;159:193–203.
34. Hasegawa H, Takano H, Zou Y, Qin Y, Hizukuri K, Odaka K, Toyozaki T, Komuro I. Pioglitazone, a peroxisome proliferator-activated receptor gamma activator, ameliorates experimental autoimmune myocarditis by modulating Th1/Th2 balance. J Mol Cell Cardiol. 2005;38:257–265.

http://www.kidney-international.org

Blockade of VEGF accelerates proteinuria, via decrease in nephrin expression in rat crescentic glomerulonephritis

A Hara[1], T Wada[1], K Furuichi[1], N Sakai[1], H Kawachi[2], F Shimizu[2], M Shibuya[3], K Matsushima[4], H Yokoyama[5], K Egashira[6] and S Kaneko[1]

[1]*Department of Gastroenterology and Nephrology, Graduate School of Medical Science, Kanazawa University, Kanazawa, Japan;* [2]*Department of Cell Biology, Institute of Nephrology, Graduate School of Medical and Dental Sciences, Niigata University, Niigata, Japan;* [3]*Department of Genetics, Institute of Medical Science, Tokyo, Japan;* [4]*Department of Molecular Preventive Medicine, Graduate School of Medicine, The University of Tokyo, Tokyo, Japan;* [5]*Division of Blood Purification, Kanazawa University, Kanazawa, Japan and* [6]*The Department of Cardiovascular Medicine, Graduate School of Medical Sciences, Kyushu University, Fukuoka, Japan*

Vascular endothelial growth factor (VEGF) is a potent angiogenic factor that maintains the glomerular and peritubular capillary (PTC) network in the kidney. The soluble form of the VEGF receptor-1 (soluble fms-like tyrosine kinase 1 (sFlt-1)) is known to regulate VEGF activity by binding VEGF in the circulation. We hypothesized that VEGF may be beneficial for maintaining glomerular filtration barrier and vascular network in rats with progressive glomerulonephritis (GN). For blockade of VEGF activity *in vivo*, rats were transfected twice with plasmid DNA encoding the murine sFlt-1 gene into femoral muscle 3 days before and 2 weeks after the induction of antiglomerular basement membrane antibody-induced GN. Inhibition of VEGF with sFlt-1 resulted in massive urinary protein excretion, concomitantly with downregulated expression of nephrin in nephritic rats. Further, blockade of VEGF induced mild proteinuria in normal rats. Administration of sFlt-1 affected neither the infiltration of macrophages nor crescentic formation. In contrast, treatment of sFlt-1 accelerated the progression of glomerulosclerosis and interstitial fibrosis accompanied with renal dysfunction and PTC loss at day 56. VEGF may play a role in maintaining the podocyte function as well as renal vasculature, thereby protecting glomeruli and interstitium from progressive renal insults.

Kidney International (2006) **69,** 1986–1995. doi:10.1038/sj.ki.5000439; published online 26 April 2006

KEYWORDS: VEGF; proteinuria; podocyte; nephrin; anti-GBM disease

Correspondence: *T Wada, Department of Gastroenterology and Nephrology and Division of Blood Purification, Graduate School of Medical Science, Kanazawa University, 13-1 Takara-machi, Kanazawa 920-8641, Japan. E-mail: twada@medf.m.kanazawa-u.ac.jp*

Received 16 June 2005; revised 26 January 2006; accepted 15 February 2006; published online 26 April 2006

Vascular endothelial growth factor (VEGF) is a potent angiogenic factor that induces endothelial cell migration, growth, differentiation, and regeneration through its receptors, vascular endothelial growth factor receptor (VEGFR)-1 (Flt-1) and VEGFR-2 (KDR/Flk-1).[1] In kidney, VEGF is abundantly expressed in glomerular epithelial cells (podocytes) and tubular epithelial cells, whereas the glomerular and peritubular capillary (PTC) endothelial cells express cognate VEGF receptors.[2–4] The importance of VEGF in kidney is evidenced by the fact that deficiency in VEGF selectively in the podocytes showed impaired glomerular capillary formation owing to a loss of endothelial cells in mice,[5] and antagonizing circulating VEGF caused glomerular endotheliosis in pregnant rats, which is also noted in human pre-eclampsia.[6]

In addition to the impacts of VEGF on endothelial cells, physiological levels of VEGF are pivotal for maintaining glomerular filtration barrier. In this regard, Sugimoto *et al.* reported that anti-VEGF antibodies and soluble VEGF receptor 1 (soluble fms-like tyrosine kinase 1 (sFlt-1)), which inhibit VEGF activity by directly sequestering VEGF and by functioning as a dominant-negative inhibitor against VEGF receptors,[7] respectively, induced proteinuria associated with podocyte dysfunction in normal kidneys.[8] Recent reports from human clinical cancer trials using anti-VEGF antibodies (Bevacizumab) suggest that proteinuria may be associated with treatment protocols.[9–11]

Therefore, we hypothesized in this study that VEGF may be responsible for maintaining the glomerular filtration barrier and vascular network in rats with progressive glomerulonephritis (GN). Molecular and pathological mechanisms involved in the increased levels of urinary protein, electron microscopic findings, and the expression of slit diaphragm-associated molecules were examined. Further, the effect of inhibition of VEGF on podocyte-associated molecules was examined. The present study shows that blockade of VEGF activity by transfection of the plasmid DNA encoding sFlt-1

gene in femoral muscles resulted in massive urinary protein excretion, concomitantly with downregulated expression of nephrin, which is one of the major glomerular slit diaphragm-associated molecules,[12] in diseased glomeruli. Treatment with sFlt-1 affected the progression of glomerulosclerosis and interstitial fibrosis, resulting in renal dysfunction. These results suggest that VEGF may play a role in maintaining the podocyte function as well as renal vasculature, thereby regulating urinary protein excretion and protecting glomeruli and interstitium from progressive insults.

RESULTS

Expression of sFlt-1

Muscle fibers positive for sFlt-1 were observed in femoral muscles from the sFlt-1 gene-transfected rats 6 days after disease induction (Figure 1a). In contrast, sFlt-1 protein was not detected in the muscles from the empty plasmid-treated rats (Figure 1b). Further, reverse transcription-polymerase chain reaction (RT-PCR) analysis of muscle tissue for sFlt-1 mRNA showed that sFlt-1 mRNA was expressed at the injected sites in sFlt-1-treated rats (Figure 1c). Finally, urinary levels of sFlt-1 increased at day 6 in rats treated with sFlt-1 compared with those from vehicle-treated rats (Figure 1d), and remained elevated for at least 14 days (data not shown).

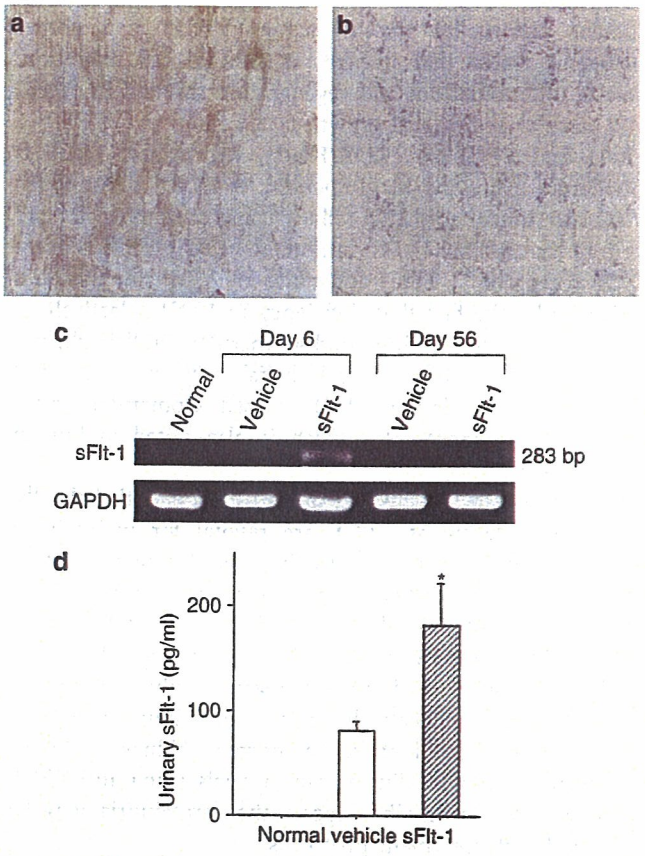

Figure 1 | sFlt-1 expression in femoral muscle. The expression of sFlt-1 in skeletal muscles, where gene transfer was performed with electroporation, was detected by an immunohistochemical method. (**a**) Fibers positive for sFlt-1 were observed in the femoral muscle from the plasmid DNA encoding sFlt-1-transfected rats 6 days after induction of GN. (**b**) There was no staining for sFlt-1 in the muscles from rats transfected with empty plasmid. sFlt-1 mRNA in muscles was determined by RT-PCR analysis. (**c**) sFlt-1 mRNA was detected in muscles 6 days after induction of GN, and barely detected 56 days after induction of GN. (**d**) Urinary levels of sFlt-1 increased 6 days after disease induction in sFlt-1-treated rats. Original magnification, × 100. *$P<0.05$ compared with rats transfected with empty plasmid.

Histopathological studies

Semiquantitative evaluation of deposition showed no significant difference in the deposition of rabbit immunoglobulin (Ig)G, rat IgG, or rat C3 between glomeruli from rats administered sFlt-1 gene or empty plasmid only (data not shown). These results suggest that induction of GN was equivalent in the two groups.

Glomerular lesions showed endocapillary proliferation, severe necrotizing lesions, and crescentic formation at day 6. Numbers of ED-1-, proliferating cell nuclear antigen-, and CD8-positive cells did not significantly differ by the administration of sFlt-1 gene at day 6. Similarly, there was no significant difference between sFlt-1- and vehicle-treated rats in formation of crescentic lesions and the number of total glomerular cells at day 6 (Table 1).

Vehicle-treated nephritic animals showed a marked degree of glomerulosclerosis, as well as interstitial fibrosis at day 56 (Figure 2a–d). sFlt-1-treated rats showed significantly more glomerulosclerosis and interstitial fibrosis at day 56.

Effects of VEGF blockade on urinary protein excretion and renal function

Ten normal untreated rats excreted minute amounts of protein in the urine. Blockade of VEGF-induced mild proteinuria by day 6 in six normal rats without anti-GBM serum, which was maintained for 28 days, but returned to nearly normal levels at day 56 (Figure 3). In contrast, all nephritic rats injected with empty plasmid excreted markedly elevated amounts of protein in the urine at days 6, 14, and 56. The administration of sFlt-1 gene significantly increased proteinuria at days 14 and 56 compared with vehicle-treated rats (Figure 3). Nephritic rats with inhibition of VEGF showed hypoproteinemia, evidenced by reduced serum total protein levels and massive ascites at killing (Figure 4a). At day

Table 1 | Effects of inhibition of VEGF activity via sFlt-1 on histopathological changes on day 6[a]

	Normal	Vehicle	sFlt-1	*P*-value[b]
Crescentic formation (%)	0	37.3±2.7	36.4±5.4	0.88
Total cell number[c]	55.3±1.1	109.2±1.5	113.5±1.6	0.09
PCNA-positive cells[c]	1.8±0.5	7.0±0.2	7.1±0.4	0.88
ED-1-positive cells[c]	0.8±0.1	13.9±0.5	13.4±0.7	0.52
CD8-positive cells[c]	0.2±0.02	1.9±0.1	1.9±0.1	0.89

Abbreviations: PCNA, proliferating cell nuclear antigen; sFlt-1, soluble *fms*-like tyrosine kinase 1; VEGF, vascular endothelial growth factor.
[a]Values are given as mean±s.e.m. $n=4$ in normal group, $n=5$ in vehicle group, and $n=4$ in sFlt-1 group.
[b]Statistical analyses are based on unpaired Student's *t*-test and Kruskal–Wallis test.
[c]Number of cells/glomerular cross-section.

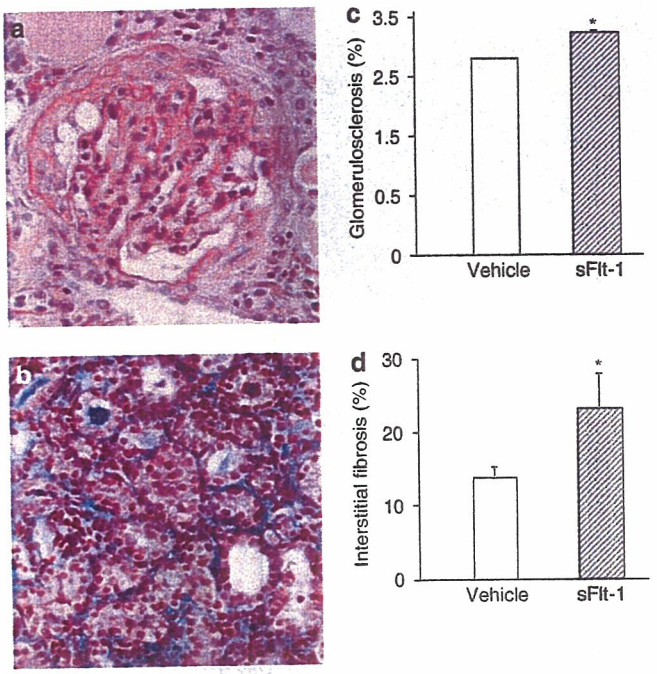

Figure 2 | VEGF inhibition accelerated glomerulosclerosis and interstitial fibrosis. Progressive renal lesions exhibited (**a**, **c**) glomerulosclerosis and (**c**, **d**) interstitial fibrosis in rats transfected with empty plasmid at day 56. In contrast, sFlt-1 treatment accelerated renal pathology. (**c**) Glomerulosclerosis and (**d**) interstitial fibrosis were more prominent. Original magnification, ×200. *$P<0.05$ compared with rats transfected with empty plasmid.

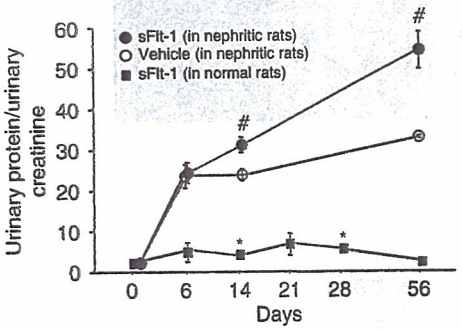

Figure 3 | Increased urinary protein excretion by inhibition of VEGF activity. Treatment of normal rats with sFlt-1 induced mild proteinuria, and its levels were maintained for 28 days and were decreased by (■) day 56. *$P<0.01$ compared with a level of proteinuria at day 0. Results from rats administered with (○) empty plasmid and (●) sFlt-1. Administration of sFlt-1 markedly increased proteinuria. #$P<0.05$ compared with rats transfected with empty plasmid.

56, animals with empty plasmid developed renal dysfunction as evidenced by increased blood urea nitrogen levels. However, inhibition of VEGF by administration of sFlt-1 gene increased blood urea nitrogen levels (Figure 4b). Serum creatinine levels in sFlt-1-treated rats tended to increase compared with those in vehicle-treated rats at day 56, but the difference was not statistically significant.

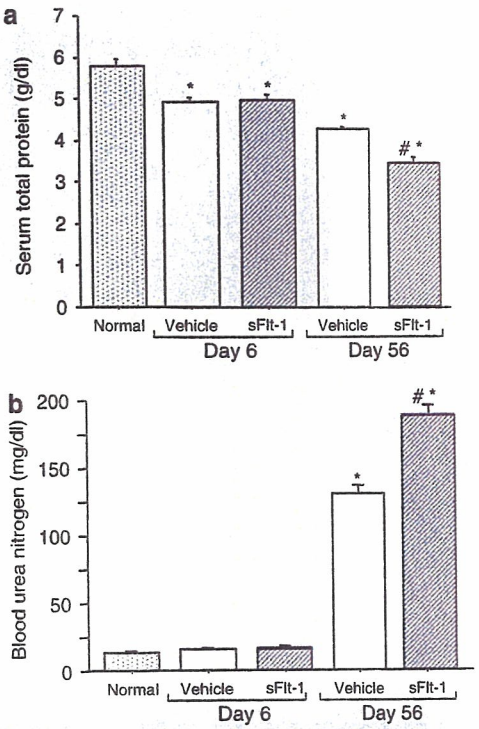

Figure 4 | Decreased serum total protein levels and deterioration of renal function by sFlt-1 treatment. (**a**) Serum total protein levels were decreased in sFlt-1-treated rats at day 56. *$P<0.05$ compared with normal rats. #$P<0.05$ compared with vehicle-treated rats. (**b**) Rats treated with sFlt-1 developed renal dysfunction, evidenced by increased blood urea nitrogen levels at day 56. *$P<0.001$ compared with normal rats. #$P<0.05$ compared with vehicle-treated rats.

Effects of VEGF blockade on glomerular epithelial cells and slit diaphragm-associated molecules

Epithelial foot processes tended to fuse in all tufts at day 6 in diseased glomeruli from rats treated with empty plasmid (Figure 5a; white arrow). In nephritic rats treated with sFlt-1, more severe fusion of epithelial foot processes occurred, and podocyte foot processes could be identified hardly (Figure 5b; black arrow). Podocytes in normal kidneys had faint desmin expression. In contrast, desmin was expressed by podocytes in nephritic rats and its expression was increased in sFlt-1-treated rats both at days 6 and 56 (Figure 5c and d).

mRNA expression of nephrin was specifically decreased by the inhibition of VEGF (Figure 5e). Nephrin protein, evaluated immunohistochemically in normal kidneys, was detected in a linear pattern along glomerular capillary walls (Figure 5f). Compared with rats treated with empty plasmid (Figure 5g), nephrin protein was reduced in sFlt-1-treated rats (Figure 5h). Concomitantly, Western blot analysis for nephrin protein revealed that nephrin was reduced in nephritic rats and that the reduction was more severe in rats treated with sFlt-1 (Figure 5i). In addition, nephrin was faintly expressed in both sFlt-1- and empty plasmid-treated rats at day 56.

In contrast to nephrin expression, expression of podocin, podoplanin, and podocalyxin did not change by the treat-

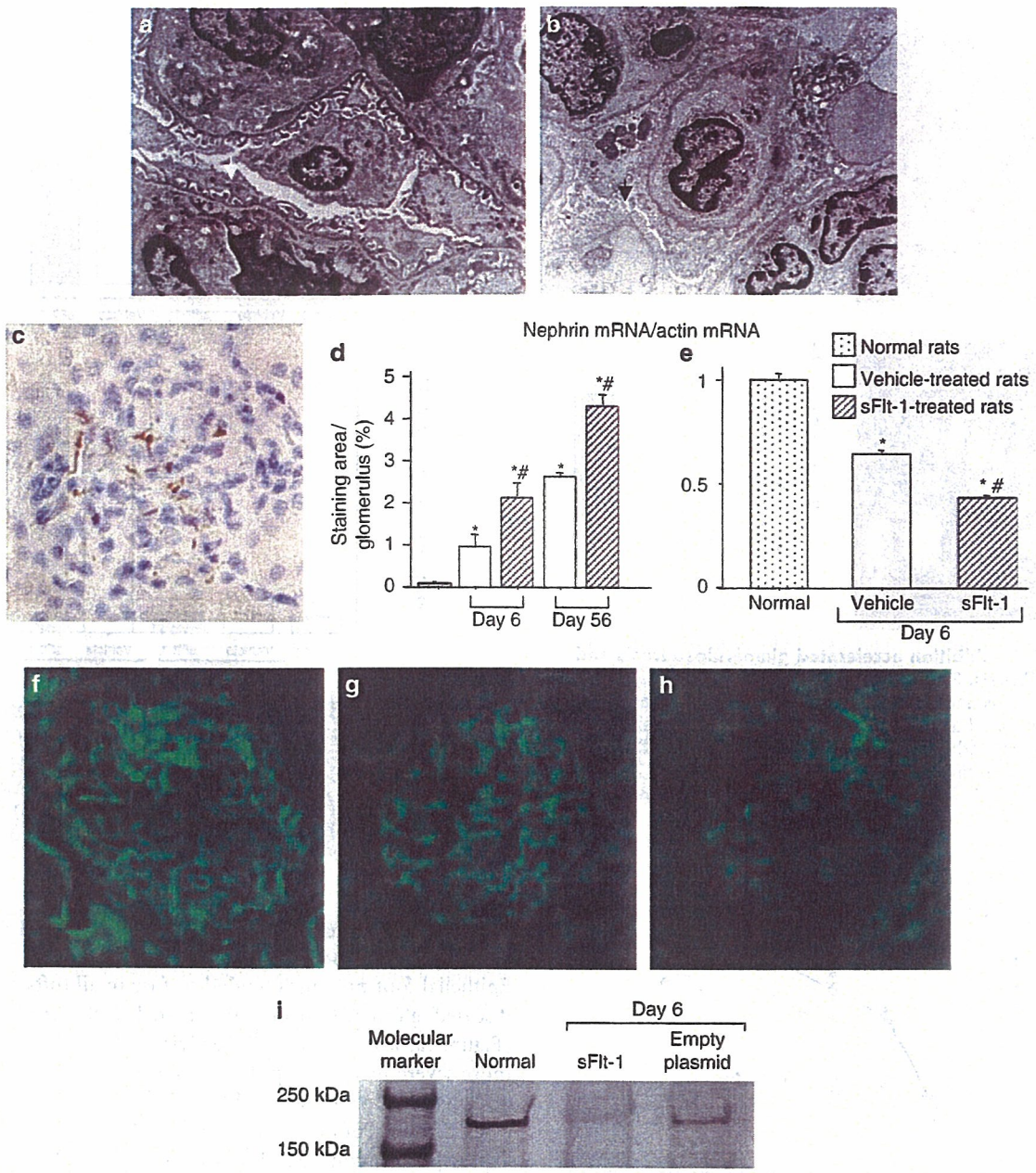

Figure 5 | Effects of anti-GBM GN and sFlt-1 treatment on podocytes and nephrin. (**a**) Podocyte foot processes fused in all tufts at day 6 in diseased glomeruli from rats transfected with empty plasmid. (**b**) sFlt-1 treatment accelerated fusion of podocyte foot processes. Original magnification, × 3000. (**c**) Expression of desmin at day 6 in diseased glomeruli from rats with empty plasmid. (**d**) Increased desmin expression in podocytes was observed in sFlt-1-treated rats at days 6 and 56. Original magnification, × 400. (**e**) mRNA expression of nephrin in normal and diseased kidneys. Expression of nephrin mRNA was decreased in anti-GBM GN and further downregulated by sFlt-1 treatment. $^{*}P<0.05$ compared with normal rats. $^{\#}P<0.05$ compared with vehicle-treated rats. Immunofluorescent microscopic findings of nephrin in (**f**) normal rats and (**g**) rats with empty plasmid. Nephrin expression was reduced at day 6. (**h**) Nephrin expression was further reduced in sFlt-1-treated rats compared with rats with empty plasmid at day 6. Original magnification, × 200. (**i**) sFlt-1 treatment markedly downregulated nephrin in diseased glomeruli as shown by Western blot analyses. Molecular markers are shown in the left lane. Data are representative of three experiments.

ment with sFlt-1 in either mRNA levels (Figure 6a–c) or protein levels (Figure 6d–g).

Microvascular changes associated with blockade of VEGF

In normal kidneys, thrombomodulin (TM)-positive glomerular and PTC endothelial cells were preserved (Figure 7a). Six days after disease induction, sFlt-1-treated rats (Figure 7c and d) had more severe TM-positive glomerular endothelial cell loss than that observed in rats injected with empty plasmid (Figure 7b and d). sFlt-1-treated rats tended to have decreased areas of TM-positive PTC endothelial cells compared with rats injected with empty plasmid at day 6 (Figure 7e).

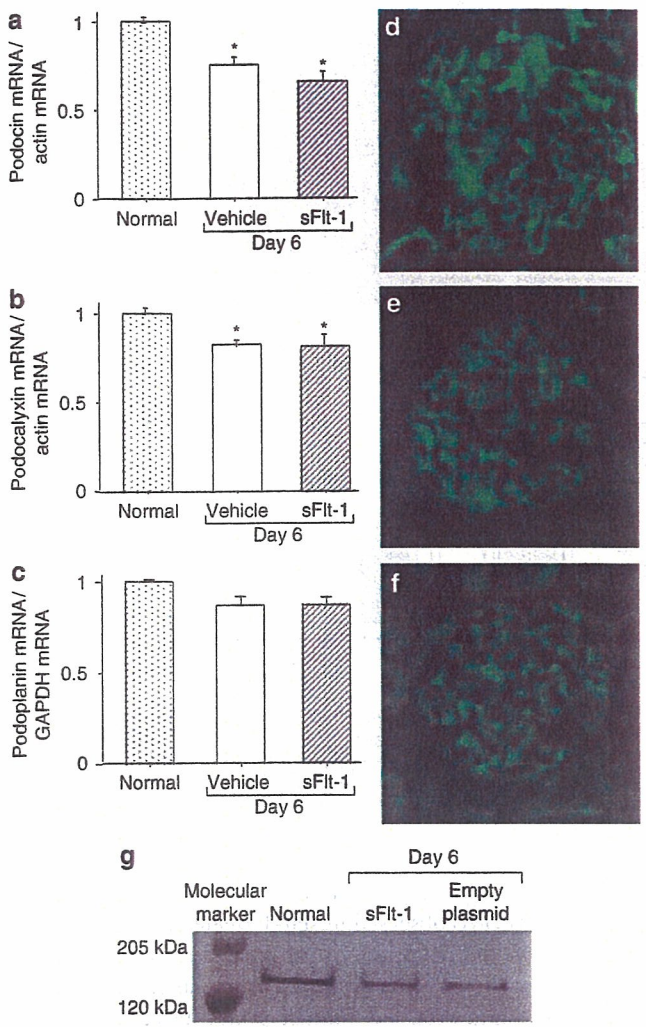

Figure 6 | Effects of anti-GBM GN and sFlt-1 treatment on podocyte-associated molecules. mRNA expression of (**a**) podocin, (**b**) podocalyxin, and (**c**) podoplaninwas decreased by anti-GBM GN and sFlt-1 treatment did not have impact on mRNA expression of these three podocyte-associated molecules. $^{*}P<0.05$ compared with normal rats. (**d**) Immunofluorescent microscopic findings of podocalyxin in normal rats. (**e**) Podocalyxin expression was reduced at day 6 in nephritic rats transfected with empty plasmid, which was not different from that in (**f**) sFlt-1-treated rats. Original magnification, × 200. (**g**) sFlt-1 treatment did not alter the podocalyxin expression in diseased glomeruli revealed by Western blot analyses. Molecular markers are shown in the left lane. Data are representative of three experiments.

Expressions of VEGF and its receptors, Flk-1 and Flt-1, in normal and diseased kidneys

mRNA expression of three isoforms of VEGF in kidneys was reduced in crescentic GN, and was further reduced by the inhibition of VEGF (Figure 8a and b). In addition, these three isoforms of VEGF were only faintly expressed in both sFlt-1- and empty plasmid-treated rats at day 56 (Figure 8a and b). VEGF protein was detected on podocytes in normal kidneys by immunohistochemistry (Figure 8c). Compared with rats treated with empty plasmid (Figure 8d), sFlt-1-treated rats had reduced VEGF protein at day 6 (Figure 8e). VEGF receptor, Flk-1, was detected in all glomeruli and PTC endothelial cells in normal rat (Figure 8f). Six days after induction of nephritis, the area of glomerular and tubulointerstitial tissue expressions of Flk-1 was decreased compared with normal rats (Figure 8g, h, l and m). At day 56, Flk-1 expression in glomeruli and interstitium was reduced via VEGF blockade (Figure 8l and m). Similarly, the expression of Flt-1 in diseased kidneys was barely detectable, whereas it was readily detected in podocytes in normal kidneys (Figure 8i–k).

DISCUSSION

This study demonstrates that administration of sFlt-1, a selective and potent inhibitor of VEGF, accelerates proteinuria with massive ascites, glomerulosclerosis, and interstitial fibrosis in rat crescentic GN, and is associated with loss of a slit diaphragm-associated molecule, nephrin, and endothelium. In this study, sFlt-1 gene transfected in femoral muscles was expressed at injected sites at mRNA and protein levels and was released to circulation, from which it translocated to urinary space beyond the glomerular basement membrane (GBM) in diseased kidneys.[7,13] This study suggests that VEGF in rats with crescentic GN may be important for maintaining renal vasculature and preventing proteinuria via regulation of nephrin, VEGF appears to protect the kidney from renal insults.

Blockade of VEGF accelerated proteinuria and reduced specifically nephrin. Nephrin, a product of the NPHS1 gene whose mutations cause congenital nephrotic syndrome of the Finnish type, is exclusively expressed by glomerular podocytes within the kidney and is localized to the podocyte slit diaphragm.[12,14] Recently, it has been reported that nephrin not only is a key slit diaphragm component but also prevents podocyte apoptosis.[15] Mice injected with anti-VEGF antibody or sFlt-1 developed proteinuria accompanied by disruption/loss of slit diaphragm and specific nephrin downregulation.[8] Therefore, one explanation for decreased expression of podocyte-associated molecules is that as a result of anti-GBM antibody-induced GN, podocyte damage occurred and progressed, followed by decreased expression of nephrin. Moreover, treatment with VEGF results in decreased urinary protein excretion and renal dysfunction.[16] Until now, the beneficial effect of VEGF on podocytes was thought to be mediated indirectly by improvement of glomerular endothelial cell survival, because podocytes were not known to express VEGF receptors. However, in addition to this paracrine role of VEGF in the glomerulus, it is possible that VEGF has an autocrine function through its tyrosine-kinase receptor that is required for podocyte survival *in vitro*.[15,17] The data suggest that VEGF maintains podocyte function and survival by regulation of nephrin, possibly acting in an autocrine and/or paracrine manner in the progressive disease.

VEGF expression was downregulated via sFlt-1 in this particular model. A recent report demonstrated that signaling through extracellular matrix proteins, in particular, laminin and its receptor $\alpha 3\beta 1$ integrin, which is highly

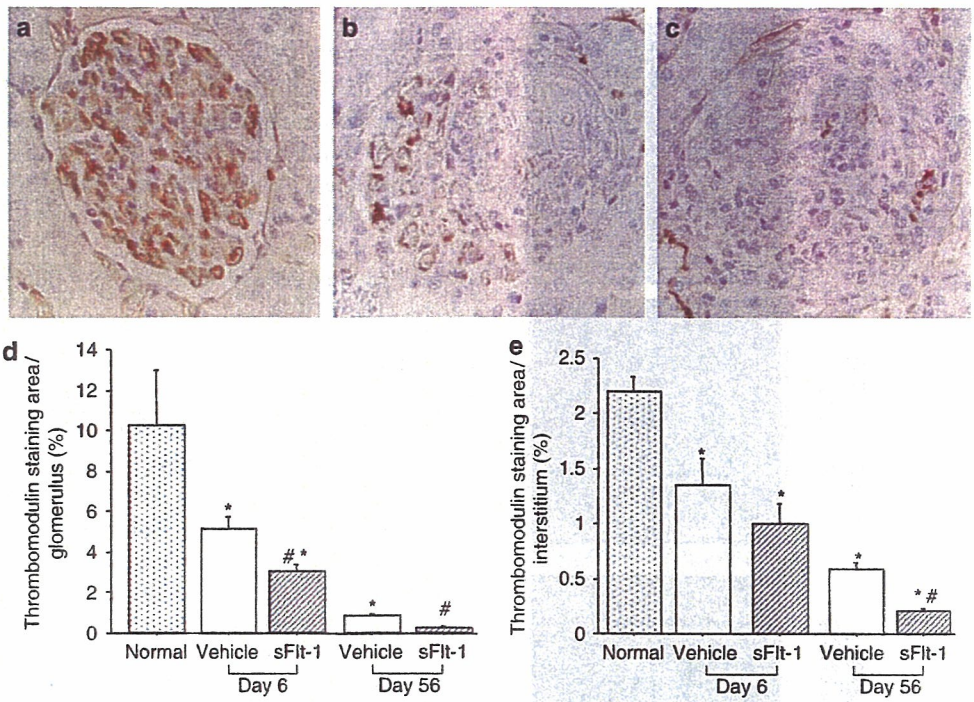

Figure 7 | VEGF inhibition accelerated glomerular and peritubular endothelial loss. (**a**) TM-positive endothelial cells were detected ubiquitously along with glomerular and peritubular capillaries in normal rats. (**b**) TM-positive endothelial cells were reduced in rats transfected with empty plasmid at day 6. (**c**) sFlt-1 treatment accelerated reduction of TM-positive endothelial cells at day 6. Original magnification, × 400. (**d**, **e**) Loss of TM-positive glomerular and peritubular endothelial cells was prominent by sFlt-1 treatment. $^{*}P < 0.05$ compared with normal rats. $^{\#}P < 0.05$ compared with vehicle-treated rats.

expressed in podocytes regulates VEGF production in cultured podocytes.[18] Hence, downregulated VEGF in this model, at least in part, is likely owing to the disturbance of the GBM matrix–podocyte interaction by anti-GBM antibodies. Further decrease in VEGF expression was observed by VEGF blockade via sFlt-1 during the course of disease. This might be explained by podocyte damage being augmented by inhibition of VEGF activity.[5,8,15,17] Therefore, downregulated VEGF in this model might perpetuate further podocyte loss and endothelial injury, thereby leading to glomerulosclerosis.

VEGF binds two related receptors, Flt-1 and KDR/Flk-1.[1,3] In rat kidney, Flk-1 has been shown to be expressed in glomerular and peritubular endothelial cells.[3] However, Flt-1 expression is controversial. In the present study, Flk-1 was locally expressed in glomerular and peritubular endothelial cells and was diminished during the disease course, concomitantly with progressive glomerular and PTC loss. Flt-1 was detected on podocytes in normal glomeruli, but was barely detected in diseased kidneys in this model. Therefore, Flk-1 appears to be the major mediator of endothelial cell mitogenesis and survival as well as angiogenesis in a crescentic GN, as reported previously.[19,20] PTC loss contributes to the etiology of the interstitial fibrosis by playing an essential role in impaired blood flow in tubular cells and interstitial cells. PTC loss may result from downregulated expression of VEGF in progressive renal diseases directly affecting PTC loss via its prosurvival effect on endothelial cells.[19,21] PTC loss may also be caused by filtered urinary proteins that lead to parenchymal damage and, eventually, renal fibrosis and dysfunction.[22] Therefore, PTC loss observed in sFlt-1-treated rats may play a crucial role in the deterioration of renal function. Recently, Flt-1 has been shown to be expressed on mesangial cells[23] and conditionally immortalized human podocyte cell line.[17] In addition, it is upregulated in certain disease models such as diabetic, passive Heymann nephritis, and puromycin aminonucleoside nephrosis.[3,24] Therefore, VEGF blockade via sFlt-1 accelerated the injury of endothelial cells as well as podocytes, mainly through the inhibition of Flk-1.

Monocytes/macrophages participate in inflammatory processes in crescentic GN. VEGF promotes monocyte chemotaxis via a primary effect on the receptor Flt-1.[25] In the present study, however, no significant effect of VEGF inhibition on crescentic formation, ED-1-positive macrophages, CD8-positive T-lymphocytes, or proliferating cell nuclear antigen-positive cells in the glomeruli was seen at day 6. These findings were consistent with the previous report that VEGF had no effect on infiltration of neutrophils, CD3-T lymphocytes, and ED-1-positive macrophages in the Thy-1/habu-snake venom GN model.[26] One plausible reason is that downregulated VEGF could not induce migration and activation of monocytes/macrophages, because VEGF-mediated chemotaxis for monocytes/macrophages depends on the dose and gradient of VEGF.[25] Therefore, although VEGF affects migration and activation of monocytes/macrophages when upregulated, such as in aortic and coronary vascular inflammation,[7,13,25,27] the residual VEGF

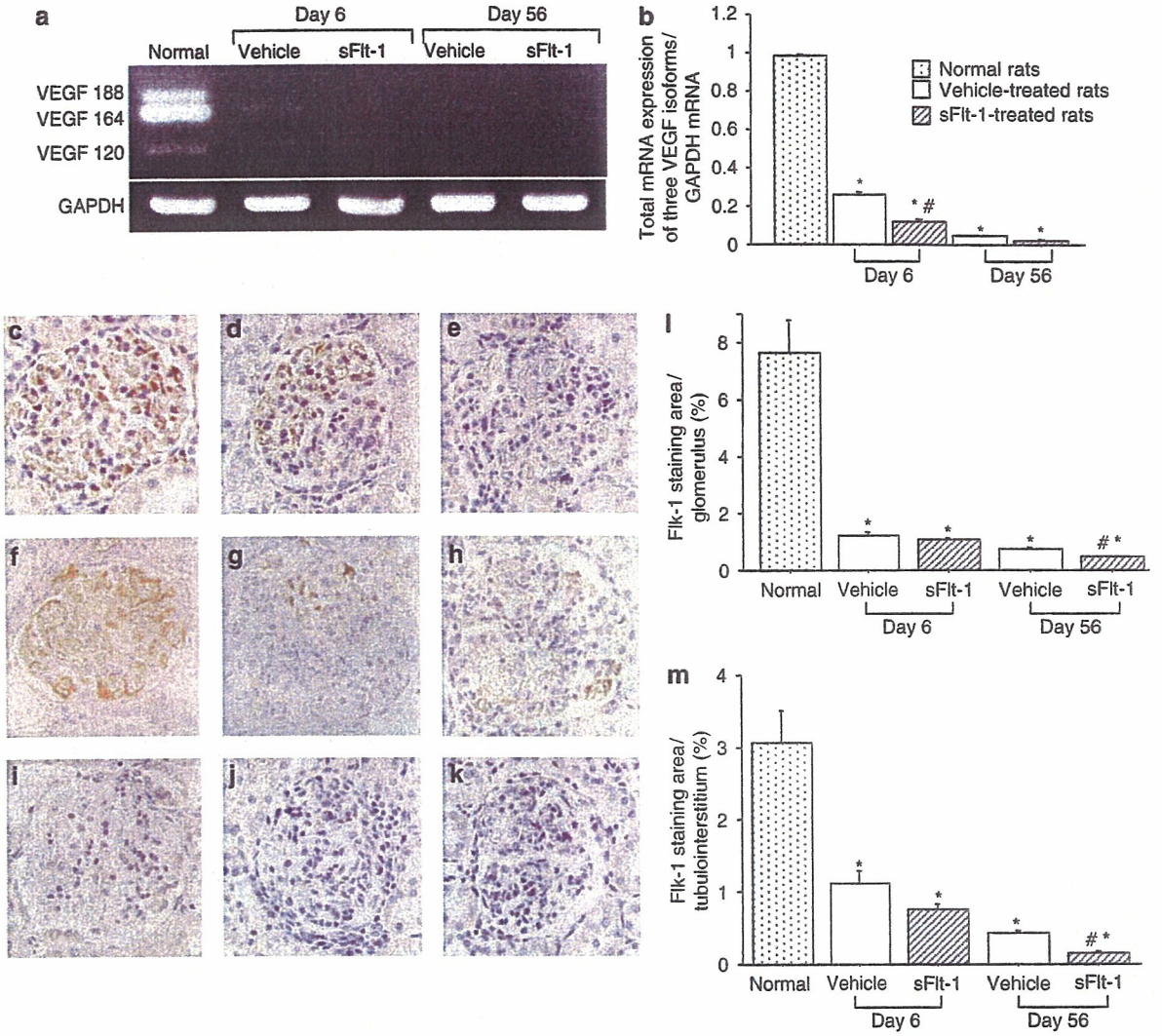

Figure 8 | Effects of anti-GBM GN and sFlt-1 treatment on expression of VEGF and VEGF receptors, Flt-1, and Flk-1. mRNA expression of VEGF in normal and diseased kidneys. (**a**) Expression of VEGF mRNA was decreased in anti-GBM GN, and further downregulated by sFlt-1 treatment. Densitometric analysis of data in (**a** and **b**). Total expression of three isoforms of VEGF mRNA in each sample is presented as a ratio to glyceraldehyde-3-phosphate dehydrogenase (GAPDH) mRNA expression in that sample. $^{*}P<0.001$ compared with normal rats. $^{\#}P<0.001$ compared with vehicle-treated rats. (**c**) VEGF was detected in podocytes in normal kidneys. (**d**) In nephritic rats, VEGF expression was reduced, and (**e**) was further decreased by sFlt-1 treatment at day 6. (**f**) Flk-1 was expressed in glomerular and peritubular endothelial cells. (**g**, **l**, and **m**) Flk-1 expression was reduced in diseased kidneys, especially in glomeruli involved with crescentic lesions at day 6. (**h**, **l**, and **m**) Flk-1 expression was more severely decreased in sFlt-1-treated rats. Flt-1 was detected on podocytes in (**i**) normal glomeruli and was hardly expressed in diseased kidneys of both (**j**) vehicle-treated and (**k**) sFlt-1-treated rats. Original magnification, ×400. $^{*}P<0.05$ compared with normal rats. $^{\#}P<0.05$ compared with vehicle-treated rats.

in this model might have no significant impact on monocytes/macrophages compared with its effects on endothelial and glomerular epithelial cells.

In conclusion, our study shows that VEGF plays a role in maintaining podocyte function as well as renal vasculature, thereby protecting glomeruli and interstitium from progressive renal insults.

MATERIALS AND METHODS

Animals

Inbred male Wistar–Kyoto rats, purchased from Charles River Japan Inc. (Atsugi, Kanagawa, Japan), aged 12 weeks were fed standard rat chow and given free access to water under 24 h light control. All the procedures used in the animal experiments complied with the standards set out in the Guideline for the Care and Use of Laboratory Animals in Takara-machi Campus of Kanazawa University.

Expression vector

The 3.3 kb mouse soluble Flt-1 gene, originally obtained from the mouse lung library,[28] was cloned into the *Bam*H1 (5′) and *Not*1 (3′) sites of the eukaryotic expression vector plasmid cDNA3.[7]

Preparation of anti-rat GBM antibodies

Rat GBM was prepared using the method of Krakower and Greenspon.[29] The preparation of anti-rat GBM antibodies was

described previously.[30] Specificity was confirmed by *in vitro* indirect immunofluorescence assays, using fluorescein isothiocyanate-conjugated anti-rabbit IgG, on frozen sections of normal Wistar rat kidneys. Sharp linear immunofluorescence was observed only along the GBM.

Experimental design

Twenty male Wistar–Kyoto rats were injected intravenously with 0.1 ml of nephrotoxic serum at day 0. Nine of 20 rats received an intramuscular injection of sFlt-1 plasmid (500 μg/150 μl phosphate-buffered saline) into the femoral muscles with a 26-G needle 3 days before injection of nephrotoxic serum, and five of nine rats received another injection of the plasmid 2 weeks thereafter. To enhance transgene expression, electroporation was performed at the injected site immediately after injection as described previously.[31,32] sFlt-1-treated rats were killed at days 6 (four rats) or 56 (five rats), and blood samples were collected. Muscle samples were obtained by partial excision of the sFlt-1-injected sites at days 6 and 56. Urine was collected 0, 6, 14, and 56 days after the nephrotoxic serum injection. The remaining 11 nephritic rats injected with empty plasmid with electroporation were also killed at days 6 (five rats) or 56 (six rats). As a control, urinary excretion of protein was measured at days 6, 14, 21, 28, and 56 in six normal rats transfected with sFlt-1 plasmid with electroporation. Levels of urinary protein excretion were determined at days 6, 14, and 56 in 10 normal untreated rats to establish normal values.

Expression of sFlt-1

The expression of sFlt-1 in skeletal muscle, which was fixed in 10% formalin followed by embedding in paraffin, was detected by immunohistochemistry using peroxidase-labeled polymer conjugated to goat anti-rabbit IgG (Envision System; DAKO Co., Carpinteria, CA, USA) and anti-Flt-1 antibodies (C-17; Santa Cruz Biotechnology, Santa Cruz, CA, USA) 6 days after disease induction.[31] Moreover, Flt-1 mRNA in femoral muscle was detected using RT-PCR. In brief, the cDNA was reverse-transcribed from 1 μg total RNA using a RT-PCR kit (Takara Shuzo, Tokyo, Japan). The cDNA product was amplified by PCR. Primers for mouse sFlt-1 (5′-GGTGCCCGCTCTTTG-3′ (sense); 5′-TGTCTCAGTGGGGATT GC-3′ (antisense)) were used to detect sFlt-1.[33] The housekeeping gene glyceraldehyde-3-phosphate dehydrogenase was used for PCR controls.

Urinary sFlt-1 measurements

The commercially available enzyme-linked immunosorbent assay kits (R&D Systems, Minneapolis, MN, USA) were used to measure mouse urinary sFlt-1 according to the manufacturer's instructions.

Histopathological studies

A portion of renal tissue was prepared as reported previously.[30] The total number of cells and number of glomeruli with crescentic formation were measured and expressed as described previously.[30] The extent of glomerular sclerosis was expressed as a percentage of the periodic acid-methanamine silver-positive area/whole glomerular area as described previously.[34] Each area was measured by a computer-aided manipulation using Mac Scope version 6.02 (Mitani Shoji Co., Ltd, Fukui, Japan). The extent of interstitial fibrosis, expressed as blue in Mallory–azan staining, was evaluated as reported previously.[32,35]

In an indirect immunoperoxidase staining, endothelial cells were detected with mouse anti-TM monoclonal antibody (141C01; NeoMarkers, Fremont, CA, USA), injured podocytes with mouse anti-desmin monoclonal antibody (D33; DAKO Co.), VEGFR-1 with goat anti-Flt-1 polyclonal antibodies (C-17; Santa Cruz Biotechnology), and VEGFR-2 with mouse anti-Flk-1 monoclonal antibody (A-3; Santa Cruz Biotechnology). In each biopsy, TM- and Flk-1-positive areas in glomeruli and tubulointerstitium were identified and expressed in a similar manner as described above, respectively.[34,35]

Another portion of renal tissue was frozen rapidly and immunostained directly with fluorescein isothiocyanate-conjugated, antiproliferating cell nuclear antigen (No. 033L245; Leinco Technologies Inc., St Louis, MO, USA) or indirectly with a mouse monoclonal antibody against rat tissue monocytes and macrophages, ED1 (IgG1; BMA Biomedicals Ltd, Augst, Switzerland) or a mouse monoclonal antibody against rat CD8 (IgG1; No. 0412; Cedarlane, Hornby, Ontario, Canada). Positive cells were counted on at least 50 randomly chosen glomeruli. Renal tissues obtained from four normal Wistar–Kyoto rats were used as negative controls. To evaluate the induction of GN, fluorescein isothiocyanate-conjugated anti-rabbit IgG (No. 38236; Organon Teknika Corporation, Durham, NC, USA), fluorescein isothiocyanate-conjugated anti-rat C3 (No. 38810; Organon Teknika Corporation), and fluorescein isothiocyanate-conjugated anti-rat IgG (No. 38731; Organon Teknika Corporation) were used.[30]

Detection of VEGF protein and its mRNA

To examine the production of VEGF in kidney before and after disease induction, immunohistochemical analysis was performed on paraffin-embedded tissue specimens with mouse anti-VEGF monoclonal antibody (C-1; Santa Cruz Biotechnology). In addition, to determine transcripts of VEGF, RT-PCR was performed using primers for VEGF (5′-GACCCTGGTGGACATCTTCCAGGA-3′ (sense); 5′-GGTGAGAGGTCTAGTTCCCGA-3′ (antisense)) with expected sizes of 514, 462, and 330 bp for amplification of VEGF188, VEGF 164, and VEGF 120, respectively.[36]

Detection of the glomerular epithelial slit diaphragm-associated molecules and extent of foot process effacement

Morphological changes of podocytes were examined by electron microscopy as described previously (Hitachi H-600, Tokyo, Japan).[30] Next, the presence of nephrin was demonstrated immunohistochemically in frozen tissue specimens with mouse anti-rat nephrin monoclonal antibody 5-1-6, and that of podocalyxin with mouse anti-podocalyxin monoclonal antibody (4D5; gift from Dr Masanori Hara).

mRNA expression of nephrin, podocin, and podocalyxin was analyzed by real-time RT-PCR on isolated cortices of kidneys from each group of rats. The cDNA was reverse-transcribed from 1 μg total RNA using SuperScript II RNase H$^-$ reverse transcriptase (Invitrogen, Carlsbad, CA, USA). Reverse transcription was performed using the following parameters: 10 min at 25°C, 30 min at 48°C, and 5 min at 95°C. In real-time PCR experiments, the Sequence Detection System (7900HT; Applied Biosystems, Foster City, CA, USA) was used. Primers for nephrin (Rn00575235, Nphs1; Applied Biosystems), podocin (Rn00709834, Nphs2; Applied Biosystems), and podocalyxin (Rn00593804, Podxl; Applied Biosystems) were used. The housekeeping gene, β-actin (Rn00667869, Actb; Applied Biosystems) was used for PCR controls. The reactions were incubated at 95°C for 10 min, followed by 40 cycles of 15 s at 95°C, 10 s at 55°C, and 20 s at 72°C. mRNA expression of nephrin,

podocin, and podocalyxin in each sample was finally described after correction with β-actin expression. In addition, expression of podoplanin mRNA was analyzed by RT-PCR. cDNA was reverse-transcribed from 1 μg total RNA using a reverse transcription-PCR kit (Takara Shuzo). Primers for podoplanin (forward: 5′-GAGCG TTTGGTTTCTGGGACTCA-3′; reverse: 5′-GGTGAGAGGTCTAGT TCCCGA-3′)[37] were used. The housekeeping gene, glyceraldehyde-3-phosphate dehydrogenase was used for PCR control. The reactions were incubated at 94°C for 3 min, followed by 35 cycles of 30 s at 94°C, 30 s at 58°C, and 60 s at 72°C.[37] Scanner analysis was examined as described previously.[32,35]

Western blot analysis

Isolated cortical portions of kidneys from each group were prepared as described elsewhere. The protein concentration of each sample was measured by Bradford Protein Assay kit (Bio-Rad Laboratories Inc., Hercules, CA, USA). The homogenate was diluted with Laemmli sample buffer (Bio-Rad Laboratories Inc.) and was boiled for 5 min and cooled on ice. Ten micrograms of protein were subjected to sodium dodecyl sulfate-polyacrylamide gel electrophoresis and electroblotted onto a polyvinylidene difluoride membrane (Bio-Rad Laboratories Inc.). The membrane was blocked with bovine serum albumin-containing TBST buffer (20 mM Tris, pH 7.6, 140 mM NaCl, and 0.1% Tween 20), and then incubated with goat anti-nephrin polyclonal antibodies (N-20; Santa Cruz Biotechnology)[38] or rabbit anti-podocalyxin polyclonal antibodies (KR064; Transgenic Co., Hyogo, Japan). To visualize the signals, the membrane was incubated with biotinylated rabbit anti-goat immunoglobulins (DAKO Co.) followed by streptavidin–horseradish peroxidase complex (DAKO Co.) for nephrin or with peroxidase-labeled polymer conjugated to goat anti-rabbit IgG (Envision System; DAKO Co.) for podocalyxin.

Determination of urinary protein, blood urea nitrogen, serum creatinine, and serum total protein concentrations

Urinary protein concentrations were determined as reported previously.[39] Urinary protein excretion was expressed as the ratio of urinary protein to urinary creatinine. Blood urea nitrogen, serum and urinary creatinine, and serum total protein levels were measured using an automated analyzer (Hitachi, Tokyo, Japan) according to the manufacturer's instructions.

Statistical analyses

The mean and standard error were calculated on all parameters determined in this study. Statistical analyses were performed using the unpaired Student's *t*-test and Kruskal–Wallis test. Values of $P<0.05$ were considered statistically significant.

ACKNOWLEDGMENTS

We gratefully thank Drs. Raghu Kalluri, Hikaru Sugimoto (Harvard Medical School), and Dr Joan Sechler (National Institute of Health) for their critical review of this paper. TW is a recipient of a Grant-in-Aid from the Ministry of Education, Science, Sports, and Culture in Japan. This work is supported in part by a Grant-in-Aid from the Ministry of Health, Labor, and Welfare of Japan.

REFERENCES

1. Ferrara N. Role of vascular endothelial growth factor in the regulation of angiogenesis. *Kidney Int* 1999; **56**: 794–814.
2. Simon M, Rockl W, Hornig C *et al.* Receptors of vascular endothelial growth factor/vascular permeability factor (VEGF/VPF) in fetal and adult human kidney: localization and [^{125}I] VEGF binding sites. *J Am Soc Nephrol* 1998; **9**: 1032–1044.
3. Schrijvers BF, Flyvbjerg A, DeVriese AS. The role of vascular endothelial growth factor (VEGF) in renal pathophysiology. *Kidney Int* 2004; **65**: 2003–2017.
4. Kitamoto Y, Tokunaga H, Tomita K. Vascular endothelial growth factor is an essential molecule for mouse kidney development: glomerulogenesis and nephrogenesis. *J Clin Invest* 1997; **99**: 2351–2357.
5. Eremina V, Sood M, Haigh J *et al.* Glomerular-specific alterations of VEGF-A expression lead to distinct congenital and acquired renal diseases. *J Clin Invest* 2003; **111**: 707–716.
6. Maynard SE, Min JY, Merchan J *et al.* Excess placental soluble fms-like tyrosine kinase 1 (sFlt-1) may contribute to endothelial dysfunction, hypertension, and proteinuria in preeclampsia. *J Clin Invest* 2003; **111**: 649–658.
7. Zhao Q, Egashira K, Inoue S *et al.* Vascular endothelial growth factor is necessary in the development of arteriosclerosis by recruiting/activating monocytes in a rat model of long-term inhibition of nitric oxide synthesis. *Circulation* 2002; **105**: 1110–1115.
8. Sugimoto H, Hamano Y, Charytan D *et al.* Neutralization of circulating Vascular endothelial growth factor (VEGF) by anti-VEGF antibodies and soluble VEGF receptor 1 (sFlt-1) induces proteinuria. *J Biol Chem* 2003; **278**: 12605–12608.
9. Kabbinavar F, Hurwits HI, Fehrenbacher L *et al.* Phase II, randomized trial comparing bevacizumab plus fluorouracil (FU)/leucovorin (LV) with FU/LV alone in patients with metastatic colorectal cancer. *J Clin Oncol* 2003; **21**: 60–65.
10. Yang JC, Haworth L, Sherry RM *et al.* A randomized trial of bevacizumab, an anti-vascular endothelial growth factor antibody, for metastatic renal cancer. *N Engl J Med* 2003; **349**: 427–434.
11. Hurwitz H, Fehrenbacher L, Novotny W *et al.* Bevacizumab plus irinotecan, fluorouracil, and leucovorin for metastatic colorectal cancer. *N Engl J Med* 2004; **350**: 2335–2342.
12. Pavenstadt H, Kriz W, Kretzler M. Cell biology of the glomerular podocyte. *Physiol Rev* 2003; **83**: 253–307.
13. Zhao Q, Ishibashi M, Hiasa K *et al.* Essential role of vascular endothelial growth factor in angiotensin II-induced vascular inflammation and remodeling. *Hypertension* 2004; **44**: 1–7.
14. Kestila M, Lenkkeri U, Mannikko M *et al.* Positionally cloned gene for a novel glomerular protein-nephrin is mutated in congenital nephrotic syndrome. *Mol Cell* 1998; **1**: 575–582.
15. Foster RR, Saleem MA, Mathieson PW *et al.* Vascular endothelial growth factor and nephrin interact and reduce apoptosis in human podocytes. *Am J Physiol Renal Physiol* 2005; **288**: F48–F57.
16. Shimizu A, Masuda Y, Mori T *et al.* Vascular endothelial growth factor165 resolves glomerular inflammation and accelerates glomerular capillary repair in rat anti-glomerular basement membrane glomerulonephritis. *J Am Soc Nephrol* 2004; **15**: 2655–2665.
17. Rebecca RF, Rachel H, Karen A *et al.* Functional evidence that vascular endothelial growth factor may act as an autocrine factor on human podocytes. *Am J Physiol Renal Physiol* 2003; **284**: F1263–F1273.
18. Datta K, Li J, Karumanchi SA *et al.* Regulation of vascular permeability factor/vascular endothelial growth factor (VPF/VEGF-A) expression in podocytes. *Kidney Int* 2004; **66**: 1471–1478.
19. Ohashi R, Shimizu A, Masuda Y *et al.* Peritubular capillary regression during the progression of experimental obstructive nephropathy. *J Am Soc Nephrol* 2002; **13**: 1795–1805.
20. Yuan HT, Tipping PG, Li XZ *et al.* Angiopoeitin correlates with glomerular capillary loss in anti-glomerular basement membrane glomerulonephritis. *Kidney Int* 2002; **61**: 2078–2089.
21. Kang DH, Joly AH, Oh SW *et al.* Impaired angiogenesis in the remnant kidney model: I. Potential role of vascular endothelial growth factor and thrombospondin-1. *J Am Soc Nephrol* 2001; **12**: 1434–1447.
22. Remuzzi G, Bertani T. Pathophysiology of progressive nephropathies. *N Engl J Med* 1998; **339**: 1448–1456.
23. Thomas S, Vanuystel J, Gruden G *et al.* Vascular endothelial growth factor receptors in human mesangium *in vitro* and in glomerular disease. *J Am Soc Nephrol* 2000; **11**: 1236–1243.
24. Kanellis J, Levidiotis V, Khong T *et al.* A study of VEGF and its receptors in two rat models of proteinuria. *Nephron Physiol* 2004; **96**: 26–36.
25. Barleon B, Sozzani S, Zhou D *et al.* Migration of human monocytes in response to vascular endothelial growth factor (VEGF) is mediated via the VEGF receptor flt-1. *Blood* 1996; **87**: 3336–3343.
26. Masuda Y, Shimizu A, Mori T *et al.* Vascular endothelial growth factor enhances glomerular capillary repair and accelerates resolution of experimentally induced glomerulonephritis. *Am J Pathol* 2001; **159**: 599–608.

27. Celletti FL, Waugh JM, Amabile PG *et al.* Vascular endothelial growth factor enhances atherosclerotic plaque progression. *Nat Med* 2001; **7**: 425–429.
28. Kondo K, Hiratsuka S, Subbalakshmi E *et al.* Genomic organization of the flt-1 gene encoding for vascular endothelial growth factor (VEGF) receptor-1 suggests an intimate evolutionary relationship between the 7-Ig and the 5-Ig tyrosine kinase receptors. *Gene* 1998; **208**: 297–305.
29. Krakower C, Greenspon SA. Localization of nephrotoxic antigen within the isolated renal glomerulus. *Arch Pathol* 1951; **51**: 629–639.
30. Wada T, Yokoyama H, Furuichi K *et al.* Intervention of crescentic glomerulonephritis by antibodies to monocyte chemotactic and activating factor (MCAF/MCP-1). *FASEB J* 1996; **10**: 1418–1425.
31. Furuichi K, Wada T, Iwata Y *et al.* Gene therapy expressing amino-terminal truncated monocyte chemoattractant protein-1 prevents renal ischemia-reperfusion injury. *J Am Soc Nephrol* 2003; **14**: 1066–1071.
32. Wada T, Furuichi K, Sakai N *et al.* Gene therapy via blockade of monocyte chemoattractant protein-1 for renal fibrosis. *J Am Soc Nephrol* 2004; **15**: 940–948.
33. Nalbandian A, Dettin L, Dym M, Ravindranath N. Expression of vascular endothelial growth factor receptors during male germ cell differentiation in the mouse. *Biol Reprod* 2003; **69**: 985–994.
34. Ando Y, Moriyama T, Miyazaki M *et al.* Enhanced glomerular expression of caldesmon in IgA nephropathy and its suppression by glucocorticoid-heparin therapy. *Nephrol Dial Transplant* 1998; **13**: 1168–1175.
35. Kitagawa K, Wada T, Furuichi K *et al.* Blockade of CCR2 ameliorates progressive fibrosis in kidney. *Am J Pathol* 2004; **165**: 237–246.
36. Kim NH, Jung HH, Cha DR, Choi DS. Expression of vascular endothelial growth factor in response to high glucose in rat mesangial cells. *J Endocriol* 2000; **165**: 617–624.
37. Han GD, Koike H, Nakatsue T *et al.* IFN-inducible protein-10 has a differential role in podocyte during Thy1.1 glomerulonephritis. *J Am Soc Nephrol* 2003; **14**: 3111–3126.
38. Hou YX, Cui L, Riordan JR, Chang XB. ATP binding to the first nucleotide-binding domain of multidrug resistance protein MRP1 increases binding and hydrolysis of ATP and trapping of ADP at the second domain. *J Biol Chem* 2002; **277**: 5110–5119.
39. Wada T, Tomosugi N, Naito T *et al.* Prevention of proteinuria by the administration of anti-interleukin 8 antibody in experimental acute immune complex-induced glomerulonephritis. *J Exp Med* 1994; **180**: 1135–1140.

A third-generation, long-acting, dihydropyridine calcium antagonist, azelnidipine, attenuates stent-associated neointimal formation in non-human primates

Kaku Nakano[a], Kensuke Egashira[a], Hideo Tada[a], Yoshiro Kohjimoto[b], Yasuhiko Hirouchi[b], Shun-ichi Kitajima[b], Yasuhisa Endo[c], Xiao-Hang Li[d] and Kenji Sunagawa[a]

Background **Calcium antagonists have been shown to reduce atherogenesis and improve clinical outcomes in atherosclerotic vascular disease. No study has so far, however, addressed the effects of calcium antagonists on stent-associated neointimal formation. We therefore investigated whether a third-generation calcium antagonist, azelnidipine, attenuates in-stent neointimal formation in non-human primates.**

Method **Male cynomolgus monkeys were fed a high cholesterol diet for 4 weeks, and were randomly assigned to three groups: a vehicle group and two other groups treated with azelnidipine at 3 and 10 mg/kg per day for an additional 24 weeks ($n = 12$ each). Multi-link stents were then implanted in the iliac artery.**

Results **Azelnidipine at the high dose reduced neointimal thickness (0.25 ± 0.02 versus 0.19 ± 0.02 mm; $P < 0.05$). Azelnidipine also reduced local oxidative stress and monocyte chemoattractant protein 1 (MCP-1) expression. No difference was found between the three groups in the degrees of injury score, inflammation score, plaque neovascularization, or plasma lipid levels. Azelnidipine also reduced MCP-1-induced proliferation/migration of vascular smooth muscle cells *in vitro*.**

Conclusions **This study demonstrated for the first time that azelnidipine attenuates in-stent neointimal formation associated with the reduced expression of MCP-1 and smooth muscle proliferation/migration in the neointima. These data in non-human primates suggest potential clinical benefits of azelnidipine as a 'vasculoprotective calcium antagonist' in patients undergoing vascular interventions.** *J Hypertens* **24:1881–1889 © 2006 Lippincott Williams & Wilkins.**

Journal of Hypertension 2006, 24:1881–1889

Keywords: monocyte, neointimal hyperplasia, restenosis, smooth muscle cell

[a]Department of Cardiovascular Medicine, Graduate School of Medical Sciences, Kyushu University, Fukuoka, Japan, [b]Primate Research Center, Guandong, China, [c]Department of Applied Biology, Kyoto Institute of Technology, Kyoto, Japan and [d]Gaoyao Kangda Laboratory Animal Science and Technology, Guandong, China

Correspondence and requests for reprints to Kensuke Egashira, MD, PhD, Department of Cardiovascular Medicine, Graduate School of Medical Science, Kyushu University, 3-1-1 Maidashi, Higashi-ku, Fukuoka 812-8582, Japan
Tel: +81 92 642 5358; fax: +81 92 642 5375; e-mail: egashira@cardiol.med.kyushu-u.ac.jp

Sponsorship: This study was supported by grants-in-aid for scientific research (nos. 14657172 and 14207036) from the Ministry of Education, Science, and Culture, Tokyo, Japan, by health science research grants (Comprehensive Research on Aging and Health, and Research on Translational Research) from the Ministry of Health Labor and Welfare, Tokyo, Japan, and by the Program for the Promotion of Fundamental Studies in Health Sciences of the Organization for Pharmaceutical Safety and Research, Tokyo, Japan.

Received 19 September 2005 **Revised** 10 April 2006
Accepted 12 April 2006

Introduction

Dihydropyridine calcium antagonists have been used worldwide for patients with hypertension and atherosclerotic vascular disease. Recent clinical trials with calcium antagonists provided evidence suggesting that reducing arterial blood pressure close to normal ranges is of great importance in reducing cardiovascular events [1–4]. Notably, in the Comparison of Amlodipine versus Enalapril to Limit Occurences of Thrombosis (CAMELOT) trial [5], compared with placebo and enalapril, the third-generation calcium antagonist amlodipine was shown to reduce hospitalization as a result of unstable angina and revascularization in patients with coronary artery disease already being treated with aspirin, beta-blockers, or statins. These latest clinical trials suggest that there might be pleiotropic actions of calcium antagonists beyond blood pressure lowering. The pleiotropic actions of calcium antagonists may be distinct from pharmacological actions related to L-type calcium channel blockade, but may be attributable to their lipophilic character leading to a high affinity with membrane phospholipid of arterial wall cells such as vascular smooth muscle cells (VSMC) [6]. The vasculoprotective actions of such calcium antagonists include an improvement in endothelial function, an anti-inflammation effect, anti-oxidant function, antiproliferation of VSMC and so forth.

In animal experiments, calcium antagonists have been shown to prevent or attenuate atherosclerosis [7,8], hypertension-induced vascular remodeling [9], heart failure [10] and neointimal formation after balloon injury [11]. However, no study has so far addressed the effects of

calcium antagonists on stent-associated neointimal formation. Investigating this subject must be of clinical importance, because stent implantation is now the major revascularization technique worldwide in patients with atherosclerotic vascular disease. Although a drug-eluting stent reduces the restenosis rate in selected arterial lesions, stent-associated restenosis remains an unsolved clinical issue in high-risk lesions. The cellular mechanism of restenosis after stenting is presumed to be neointimal formation as a result of VSMC proliferation/migration, recruitment of bone marrow-derived progenitor cells or inflammation in response to injury [12–14].

Azelnidipine is a newly developed third-generation calcium antagonist and has antihypertensive action that is comparable to amlodipine [15]. Azelnidipine has strong lipophilicity and affinity to membranes of VSMC [16,17]. Therefore, the aim of this study was to investigate whether azelnidipine at a clinical dose range attenuates in-stent neointimal formation in non-human primates (cynomolgus monkeys). To gain clinical significance for the results obtained, we used a non-human primate model of stent-associated neointimal formation [12].

Materials and methods

Experimental animals

Thirty-six 5-year-old male cynomolgus monkeys weighing 4.2–6.6 kg were purchased. The study protocol was reviewed and approved by the Committee on the Ethics of Animal Experiments, Kyushu University Graduate School of Medical Sciences. The animal care before and after the operation of the animal model was performed in Gaoyao Kangda Laboratory Animal Science and Technology in China. A part of this study was performed at the Station for Collaborative Research and the Morphology Core, Kyushu University Graduate School of Medical Sciences.

Animal model of in-stent restenosis

All animals were fed a high-cholesterol diet (0.5% cholesterol and 6% corn oil) for 4 weeks before stent implantation (Fig. 1). Ticlopidine 100 mg and aspirin 81 mg were started 7 days before the initial procedure. Aspirin was to be given and continued until animals were killed at 6 months, and ticlopidine was administered for 28 days. The animals were randomly assigned to three groups as follows: (i) no treatment vehicle control group (0.5% carboxymethyl cellulose sodium salt); (ii) low-dose azeenidipine (3 mg/kg per day; donated by Sankyo Pharmaceutical Co., Tokyo, Japan) group; (iii) high-dose azelnidipine (10 mg/kg per day) group ($n = 12$ each). Azelnidipine treatment was carried out once a day by gavage for 24 weeks. One week after grouping, all monkeys were anaesthetized with ketamine hydrochloride (10 mg/kg intramuscularly) and sodium pentobarbital (30 mg/kg intravenously), and underwent the placement of a 15 mm-long Multilink stent mounted over the 3-mm balloon implanted in the iliac artery (30 s inflation at 6 atm followed by 60 s inflation at 8 atm, resulting in a stent-to-artery ratio of 1.2 : 1.0) as described [12]. After the operation, all monkeys were fed the same high-cholesterol diet.

Fig. 1

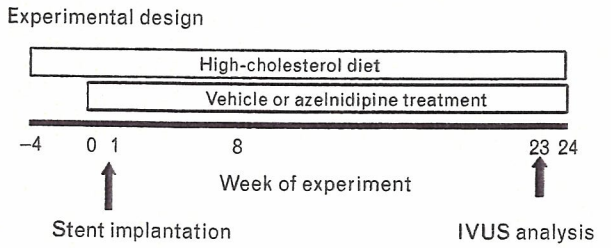

Experimental design. IVUS, Intravascular ultrasound.

Histopathology and immunohistochemistry

Stented arterial sections were excised and fixed for 24 h with 95% ethanol and 1% acetic acid. Each segment was divided into two parts at the centre of the stent. The proximal part was embedded in methyl methacrylate mixed with *n*-butyl methacrylate to allow for sectioning through metal stent struts. Serial sections were stained with elastica van Gieson and haematoxylin eosin. To evaluate the stent area, lumen area, medial area, and neointimal area, the neointimal thickening (neointimal area/length of internal elastica lamina; IEL) were measured. An immunohistochemical study was performed with antibodies against human smooth muscle actin (1A4; Dako, Tokyo, Japan) and von Willebrand factor (vWF; Dako). To evaluate the degree of neovascularization the number of arterioles in the intima and adventitia were counted.

The distal part was used for immunohistochemical analysis. After stent struts were gently removed with micro forceps, the tissue was dehydrated, embedded in paraffin, and cut into 5-μm thick slices. They were subjected to immunostaining using antibodies against human monocyte chemoattractant protein 1 (MCP-1; Santa Cruz, California, USA) and C-C chemokine receptor 2 (CCR2, Santa Cruz) as described [12]. A single observer, who was blinded to the experiment protocol, performed the morphometry. All images were captured by an Olympus microscope equipped with a digital camera (HC-2500) and were analysed using Adobe Photoshop 6.0 (Adobe Systems, San Jose, California, USA) and Scion Image 1.62 (Scion, Frederick, Maryland, USA) software.

Local oxidative stress with fluorescent dihydroethidium micrographic analysis

Frozen, enzymatically intact, sections (10-μm thick) just at the proximal edge of stented iliac arteries were incubated with dihydroethidium (10 μmol/l; Sigma, Tokyo,

Japan) in phosphate-buffered saline for 30 min at 37°C in a humidified chamber protected from light. Ethidium bromide was detected by fluorescent microscopy as described previously [18]. One representative section per artery was counted in all animals.

Intravascular ultrasound procedure and analysis

Twenty-three weeks after stent implantation, intravascular ultrasound imaging (IVUS) was performed. The imaging was performed using a 40 MHz ultrasonic imaging catheter (Ultra Cross; Boston Scientific, Boston, Massachusetts, USA) and an automatic pullback device, and the studies were recorded on 1/2-inch high-resolution s-VHS tapes for off-line volumetric assessment. IVUS analysis included stent area and proliferative intimal area.

Injury and inflammation scores

The injury and inflammatory scores were determined at each strut site, and mean values were calculated for each stented segment as previously described [19,20]. In brief, a numeric value from 0 (no injury) to 3 (most injury) was assigned: 0, endothelial denudate, IEL intact; 1, IEL lacerated, media compressed, not lacerated; 2, IEL lacerated, media lacerated, external elastica lamina compressed, not lacerated; and 3, media severely lacerated, external elastica lamina lacerated, adventitia may contain stent strut. The average injury score for each segment was calculated by dividing the sum of injury scores by the total number of struts at the examined section. The inflammation score took into consideration the extent and density of the inflammatory infiltrate in each individual strut. With regard to the inflammatory score for each individual strut, the grading is: 0, no inflammatory cells surrounding the strut; 1, light, non-circumferential inflammatory cells infiltrate surrounding the strut; 2, localized, moderate-to-dense cellular aggregate surrounding the strut non-circumferentially; and 3, circumferential dense inflammatory cells, infiltration of the strut. The inflammatory score for each cross section was calculated in the same manner as for the injury score (sum of the individual inflammatory scores, divided by the number of struts in the examined section).

Biochemical measurements

Biochemical parameters listed in Tables 1 and 2 were measured. MCP-1, interleukin (IL)-8, and transforming growth factor beta 1 were measured using commercially available enzyme-linked immunosorbent assay kits for humans (Quantikine R&D Systems, Minneapolis, Minnesota, USA). 8-Iso prostaglandin F2α (isoprostanes) in the urine was measured by high-performance liquid chromatography/tandem mass spectrometry as previously reported [21]. Isoprostanes were adjusted according to the creatinine level. Urine was collected over 3 h while each animal was in a metabolic cage.

Proliferation and migration assay in vascular smooth muscle cells

Human coronary artery VSMC (Cambrex Bio Science Walkersville Inc., Walkersville, Tennessee, USA) were

Table 1 Systemic biochemical parameters and body weight

		Week of experiment			
Parameters	Groups	0	8	16	24
Total cholesterol (mg/dl)	Vehicle control	430 ± 51	495 ± 51	417 ± 34	646 ± 55*
	Azel 3 mg/kg	470 ± 32	555 ± 62	524 ± 70	631 ± 42*
	Azel 10 mg/kg	437 ± 33	480 ± 47	347 ± 28	568 ± 50*
HDL-cholesterol (mg/dl)	Vehicle control	20 ± 2	19 ± 4	22 ± 6	14 ± 2
	Azel 3 mg/kg	18 ± 2	14 ± 2	15 ± 2	15 ± 2
	Azel 10 mg/kg	21 ± 4	14 ± 2	17 ± 4	16 ± 2
LDL-cholesterol (mg/dl)	Vehicle control	370 ± 46	387 ± 37	315 ± 28	512 ± 39*
	Azel 3 mg/kg	381 ± 31	430 ± 46	385 ± 46	466 ± 27*
	Azel 10 mg/kg	298 ± 32	381 ± 40	267 ± 24	420 ± 29*
Triglycerides (mg/dl)	Vehicle control	16 ± 3	16 ± 4	13 ± 1	18 ± 2
	Azel 3 mg/kg	10 ± 1	16 ± 3	13 ± 2	33 ± 9
	Azel 10 mg/kg	14 ± 1	25 ± 12	12 ± 2	25 ± 4
Glucose (mg/dl)	Vehicle control	58 ± 3	67 ± 3	64 ± 2	62 ± 3
	Azel 3 mg/kg	60 ± 4	60 ± 3	63 ± 3	66 ± 3
	Azel 10 mg/kg	65 ± 4	65 ± 3	61 ± 2	59 ± 3
GOT (unit/l)	Vehicle control	52 ± 6	44 ± 6	50 ± 4	54 ± 4
	Azel 3 mg/kg	51 ± 3	43 ± 3	47 ± 4	55 ± 3
	Azel 10 mg/kg	45 ± 4	41 ± 4	50 ± 6	61 ± 6
GPT (unit/l)	Vehicle control	29 ± 7	21 ± 3	20 ± 4	23 ± 2
	Azel 3 mg/kg	25 ± 2	20 ± 2	22 ± 7	23 ± 2
	Azel 10 mg/kg	21 ± 2	17 ± 2	17 ± 5	28 ± 6
Angiotensin II (pg/ml)	Vehicle control	29 ± 8	19 ± 4	14 ± 2	43 ± 10
	Azel 3 mg/kg	12 ± 2	15 ± 3	15 ± 3	21 ± 5
	Azel 10 mg/kg	12 ± 1	11 ± 2	15 ± 3	31 ± 8
Body weight (kg)	Vehicle control	5.2 ± 0.2	5.6 ± 0.2	6.1 ± 0.2	6.1 ± 0.2
	Azel 3 mg/kg	5.2 ± 0.2	5.6 ± 0.3	5.8 ± 0.3	5.8 ± 0.3
	Azel 10 mg/kg	5.2 ± 0.2	5.6 ± 0.2	6.0 ± 0.3	5.9 ± 0.3

Azel, azelnidipine; GOT, glutamic-oxaloacetic transaminase; GPT, glutamic-pyruvic transaminase; HDL, high-density lipoprotein; LDL, low-density lipoprotein. Data are mean ± SEM ($n = 12$ each). *$P < 0.05$ versus 0 week.

Table 2 Systemic oxidative stress marker and cytokines

Parameters	Groups	Week of experiment			
		0	8	16	24
8-Iso-prostaglandin in urine (ng/mg creatinine)	No treatment	716 ± 86	691 ± 94	654 ± 75	603 ± 88
	Azel 3 mg/kg	714 ± 78	572 ± 92	621 ± 86	626 ± 66
	Azel 10 mg/kg	845 ± 79	674 ± 98	693 ± 92	573 ± 78*
MCP-1 in serum (pg/ml)	No treatment	44 ± 5	40 ± 11	51 ± 3	61 ± 5*
	Azel 3 mg/kg	46 ± 3	37 ± 8	45 ± 3	47 ± 5
	Azel 10 mg/kg	47 ± 4	32 ± 7	29 ± 5†,*	37 ± 4†,*
IL-8 in serum (ng/ml)	No treatment	3.0 ± 0.3	3.8 ± 0.5	4.4 ± 0.5	3.2 ± 0.5
	Azel 3 mg/kg	2.2 ± 0.3	2.9 ± 0.3	4.6 ± 0.4	3.6 ± 0.7
	Azel 10 mg/kg	2.7 ± 0.3	3.3 ± 0.4	4.2 ± 0.8	2.7 ± 0.6
TGF-β1 in serum (ng/ml)	No treatment	63 ± 6	70 ± 7	67 ± 7	47 ± 4
	Azel 3 mg/kg	55 ± 4	67 ± 3	68 ± 7	43 ± 5
	Azel 10 mg/kg	56 ± 4	73 ± 4	62 ± 4	42 ± 3

Azel, azelnidipine; IL, interleukin; MCP-1, Monocyte chemoattractant protein 1; TGF-β1, transforming growth factor beta 1. Data are mean ± SEM ($n = 12$ each). *$P < 0.01$ versus 0 week, †$P < 0.05$ versus no treatment group.

cultured, and placed into 48-well culture plates (Falcon 354506 Biocoat Cell Ware Human Fibronectin; Bioscience Inc., Bedford Massachusetts, USA). Proliferation was stimulated by human MCP-1 at 10 ng/ml (Sigma). Azelnidipine at 1, 10, and 100 nmol or solvent were added to the wells. Four days later, the cells were fixed with methanol and a single observer, who was blinded to the experimental protocol, counted the number of cells per plate.

The migration of rat aortic smooth muscle cells was assessed with a Boyden chamber type cell migration assay kit housing a collagen-precoated polycarbonate membrane with 8.0-μm pores (Chemicon International Inc., Termacula, California, USA), as previously described [22]. The lower chambers were filled with or without human MCP-1 at 10 ng/ml (Sigma). Then cells (1×10^5 cells/ml) were placed on the upper side of the membrane and allowed to migrate through the pores. After 4 h of incubation, the number of cells that migrated to the lower surface of the membrane was counted per ×200 high-power fields. Azelnidipine at 1, 10, and 100 nmol or solvent was added to the lower chamber.

The concentrations of azelnidipine at ranges of 1–10 nmol can be considered as a clinically relevant dose, because the concentrations are nearly equivalent to the concentration reported in human subjects who were orally administered a 5 or 15 mg azelnidipine tablet [23].

Measurements of arterial blood pressure, heart rate, and plasma azelnidipine levels

Separate preliminary experiments were performed to determine the effects of azelnidipine on arterial blood pressure and heart rate in cynomolgus monkeys under conscious conditions. On the last day of the drug treatment period, blood samples were drawn before and after drug administration, and the plasma drug concentration was determined by gas chromatography–mass spectrometry [15].

Statistical analysis

Data are expressed as the mean ± SE. Statistical analysis of differences was compared by analysis of variance and Dunnet's multiple comparison tests. A P value of less than 0.05 was considered to be statistically significant.

Results

General status

No animals showed any adverse clinical signs (decreased spontaneous motor action, decreased food consumption, diarrhoea, limping and prone position, etc.) during the experimental period and all survived. There was no significant treatment effect on body weight among the groups (Table 1).

Histopathological and immunohistochemical analysis, and detection of local oxidative stress

There were no significant differences in stent area, IEL length, and medial area among all three groups (Fig. 2). Azelnidipine at the high dose tended to decrease the neointimal area (vehicle group, 2.4 ± 0.2; low-dose group, 2.3 ± 0.2; high-dose group, 1.8 ± 0.2 mm^2; vehicle versus high dose $P = 0.07$) and significantly decreased neointimal thickening (vehicle group, 0.25 ± 0.02; low-dose group, 0.24 ± 0.02; high-dose group, 0.19 ± 0.02; vehicle versus high dose $P < 0.05$; Fig. 2).

Both MCP-1 and CCR2 immunoreactivity was not detected in the non-stented normal artery (data not shown). In contrast, intense MCP-1 and CCR2 immunoreactivity was evident in the neointima and media of stented arteries from the control group. The percentage of MCP-1-positive cells in the neointima decreased in the high-dose azelnidipine group (Fig. 3), whereas the percentage of CCR2-positive cells did not differ among the three groups. In contrast, there was no significant difference in the percentage of MCP-1 or CCR2-positive cells in the media among the three groups.

Local oxidative stress was measured with dihydroethidium staining. No apparent dihydroethidium fluorescence

Fig. 2

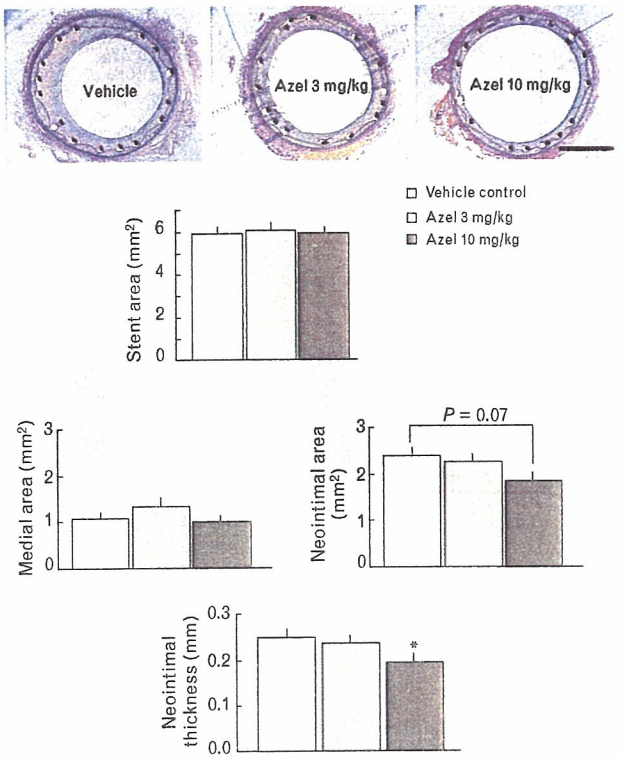

Effects of azelnidipine on stent-associated neointimal formation (histopathological analysis). (a) Representative photomicrographs of cross-sections of the stented iliac artery stained with elastica van Gieson from vehicle control group (left panel), low-dose azelnidipine (Azel) group (middle panel), and high-dose azelnidipine group (right panel) 24 weeks after stenting. Bar 1 mm. (b) Stent area (area within the stent itself), medial area (area within the external elastica lamina minus internal elastica lamina area), neointimal area (area within the internal elastica lamina minus lumen area), and neointimal thickening ($n = 12$ each). $^*P < 0.05$ versus vehicle group. Each value represents mean ± SEM.

Fig. 3

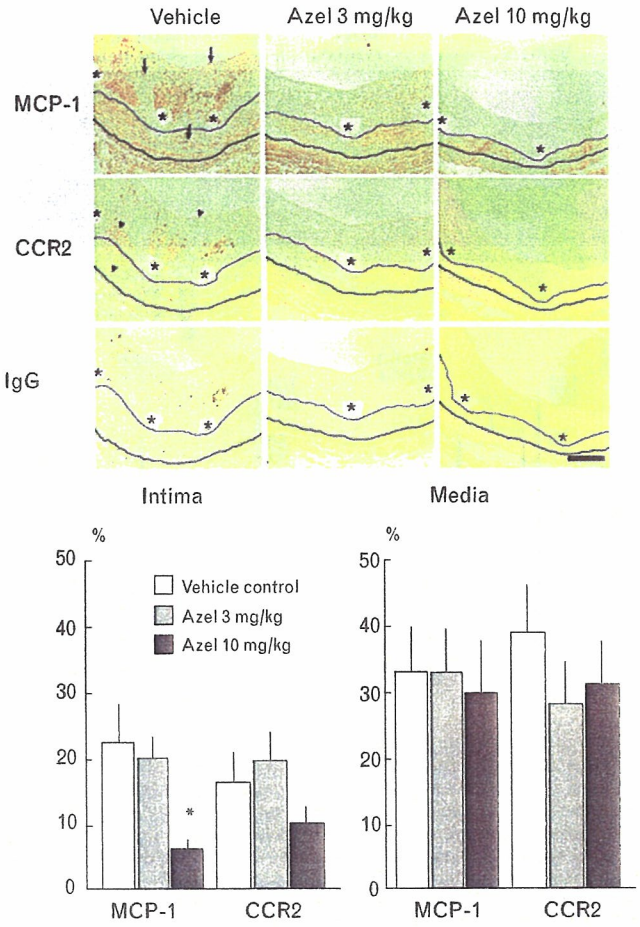

Effects of azelnidipine (Azel) on immunoreactivity for monocyte chemoattractant protein 1 (MCP-1) and C-C chemokine receptor 2 (CCR2). (a) Cross-sections of stented arteries from experimental groups stained immunohistochemically with the antibody against MCP-1 (arrows), CCR2 (arrow heads) or non-immune IgG (* indicates stent strut sites). White and blue lines show internal and external elastica lamina, respectively. (b) The percentages of MCP-1 and CCR2-positive cells in the neointima and media ($n = 12$ each). Bar 100 μm. $^*P < 0.05$ versus vehicle group. Each value represents mean ± SEM.

was detected in the non-stented normal artery (data not shown). As shown in Fig. 4, the fluorescent signal attributable to superoxide production was markedly enhanced in the neointima and media from the control group. The intensity of dihydroethidium fluorescence in the neointima decreased in the high-dose azelnidipine group, whereas the dihydroethidium signal in the media did not differ among the three groups (Fig. 4).

Injury score, inflammation score, and neovascularization

There was no significant difference in the injury score and inflammation score between the three groups (Fig. 5). Also, there were no significant differences in the degrees of neovascularization in the neointima (vWF-positive microvessels/mm^2) and adventitia (vWF-positive microvessels/section; Fig. 5).

Intravascular ultrasound imaging analysis

The degrees of neointimal formation were also investigated by IVUS analysis. As shown in histopathological analysis, high-dose azelnidipine reduced stent-associated neointimal formation by 42% (Fig. 6).

Systemic biochemical parameters

Low and high doses of azelnidipine also did not affect lipid profiles, angiotensin II and liver transaminases (Table 1). Azelnidipine at the high dose decreased 8-iso-prostaglandin F2α in urine at week 24 (Table 2). Serum levels of MCP-1 increased at week 24 in the vehicle group (Table 2). No increase in serum MCP-1 levels was noted in azelnidipine treatment groups. Notably, azelnidipine at the high dose reduced serum MCP-1 levels. In contrast, there were no treatment effects of azelnidipine on serum levels of IL-8 and transforming growth factor beta 1 (Table 2).

Fig. 4

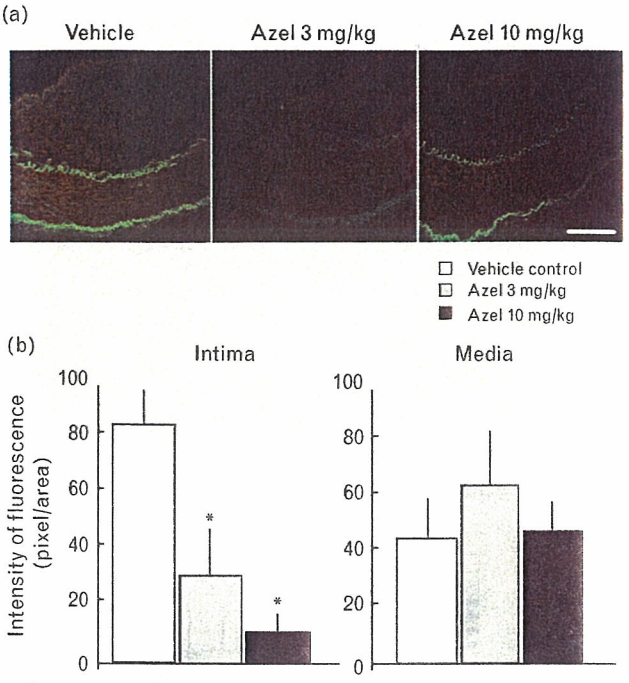

Effects of azelnidipine (Azel) on local oxidative stress marker. (a) Representative superoxide detection with dihydroethidium in cross-sections of iliac arteries. Red colour expressed dihydroethidium-stained positive nuclei, and yellow or green expressed autofluorescences. Autofluorescences were agreed internal elastica lamina (upper line) and external elastica lamina (lower line). Bar 100 μm. (b) Mean fluorescent intensity in the neointima and media ($n = 12$ each). $^*P < 0.01$ versus vehicle group. Each value represents mean ± SEM.

Fig. 5

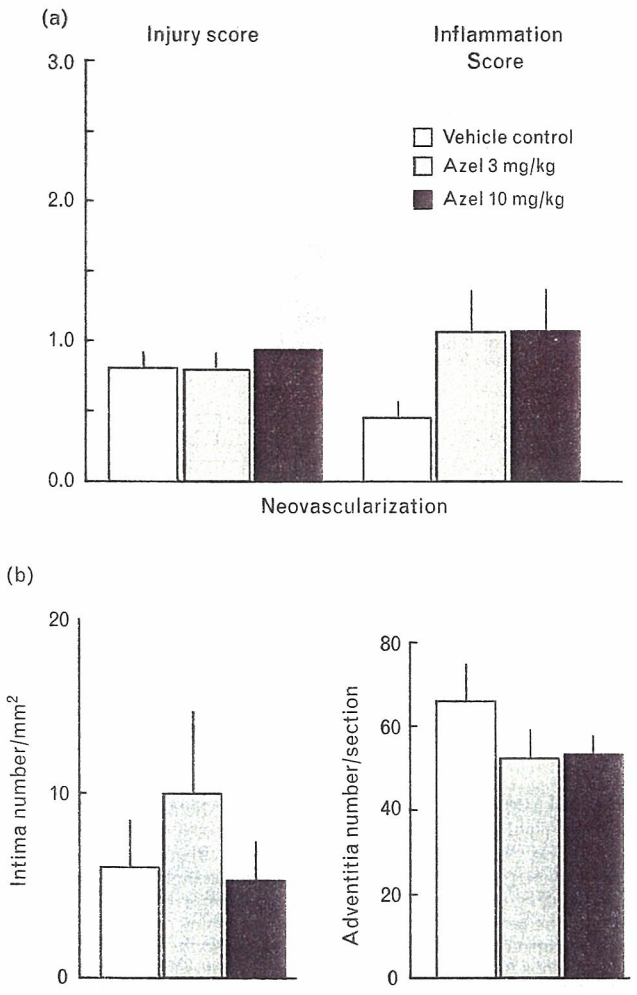

Effects of azelnidipine (Azel) on injury score, inflammation score, and neovascularization. (a) Injury score and inflammation score. (b) The degrees of neovascularization in the neointima and adventitia. The neovascularization were defined as von Willebrand factor (vWF)-positive microvessels/mm^2 in the neointima and vWF-positive microvessels/section in adventitia ($n = 12$ each). Each value represents mean ± SEM.

Proliferation and migration assay of vascular smooth muscle cells

Azelnidipine at 1, 10, and 100 nmol significantly inhibited MCP-1-induced proliferation in a dose-dependent manner (Fig. 7). Azelnidipine also reduced the MCP-1-induced migration of rat aortic smooth muscle cells (Fig. 7).

Haemodynamic parameters and plasma azelnidipine concentrations

Azelnidipine at the low and high doses did not affect haemodynamic parameters (Table 3). The maximum concentration (C_{max}) of azelnidipine at 3 and 10 mg/kg per day was 36 ± 17 and 107 ± 17 ng/ml, respectively, in monkeys. The C_{max} after oral administration of azelnidipine at 16 mg in hypertensive individuals is reported to be 48 ± 19 ng/ml [15].

Discussion

The present study demonstrated for the first time that a newly developed calcium antagonist, azelnidipine, at 10 mg/kg attenuated neointimal formation 6 months after stent implantation in hypercholesterolemic non-human primates (cynomolgus monkeys). We evaluated the degrees of stent-associated neointimal formation in two ways: histopathological and IVUS analyses. Both methods demonstrated significant benefits of azelnidipine by reducing neointimal formation after stent implantation. Although an appropriate animal model for the evaluation of stent-associated neointimal formation (restenotic changes) is uncertain, the non-human primate model may gain the advantage over non-primate animal models such as rabbits and pigs, because adequate degrees of neointima develop after stenting, and vascular inflammatory and proliferative responses to injury in non-human primates are presumed to be closer to those in humans than other non-primate models. Therefore, the use of non-human primates may allow us to evaluate the efficacy of any therapies on